ISSN: 2997-2795

Research Article

Annals of Computational Physics and Material Science

Muon Mass Model - Theoretical Masses of Tau-Lepton, u- and d-quarks in Simplified Models - General Approach to Calculate Elementary Particle Masses

Pavel Viacheslavovich Ragin*

Independent Researcher, Belarus

*Corresponding Author
Pavel Viacheslavovich Ragin, Independent Researcher, Belarus.

Submitted: 2024, Oct 25; **Accepted:** 2024, Nov 26; **Published:** 2024, Dec 06

Citation: Ragin, P. V. (2024). Muon Mass Model - Theoretical Masses of Tau-Lepton, u- and d-quarks in Simplified Models - General Approach to Calculate Elementary Particle Masses. *Ann Comp Phy Material Sci, 1*(4), 01-24.

Abstract

Numerical values of masses of elementary particles are one of the most fundamental and oldest unsolved problems (the Higgs mechanism does not explain them). In the model presented here for the first time, the theoretical mass of a "heavy electron", muon, is calculated as 206.7 (±2.5) electron masses, which is 100.0% (±1.2%) of the experimental value of 206.7682827(46). The result is obtained through 100 iterations of the algorithm, which uses random numbers (from the π sequence) to represent the uncertainty of the coordinates of interacting muon substructures. Muon is considered a structure of interconnected nodes - identical deformable balls - and contains, in contrast to a single node as a 1st-order structure (and a 1st generation particle, electron) - a layer of 12 nodes surrounding it, thus forming a 2nd-order structure, which also looks like a ball but on a smaller scale. The simplest attraction forces are modelled between the nodes, inversely proportional to the square of the distance, in equilibrium with repulsion forces arising from a relation analogous to the Heisenberg uncertainty formula. The energy-mass of the muon turns out to be equal to the total useful energy released during the structure's formation - the collapse of 13 nodes initially separated at infinity. We finish with discussing the tauon's, u- and d-quarks' masses in simplified cases, showing the generality of our approach. Some implications for future theoretical work are also given.

Keywords: Mass Spectrum of Elementary Particles, Mass Generation Mechanism, Three Generations of Particles, Muon, Leptons, Beyond the Standard Model

1. Introduction

The muon is a "heavier version" of the electron, and is an elementary particle discovered back in 1937 [1]. The muon's experimental mass, 206.7682827 (±0.0000046) electron masses, is extremely precise [2]. (Note: examples of expressing muon mass in units of electron masses are already in the literature) [3,4]. This high precision provides a strong opportunity to test models designed to explain the masses of elementary particles, including muon. Despite the existence of such models: Darling model (1950), Nambu formula (1952), Heisenberg model (mid-1950s), Horning formula (1960), Mirman equation (1961) - modifies that of Nambu, Ivanter topological model (1963), Kumar-Muthanna-Sinha model (1972), Goldman and Vinciarelli formula (1974), Mohapatra model (1974), Terazawa-Chikashige-Akama equations (1977), models of Barr and Zee (1978), Georgi-Nanopoulos formula (1979), Georgi and Jarlskog model (1979), Nambu-Barut equation (1979) - Nambu formula modification, model of Barbieri and Nanopoulos (1980), Terazawa model (1980), two Koide formulas (1981), Barricelli equation (1981), later models (including similar to the Nambu formula and Nambu-Barut equation, and that modify one of the Koide formulas), and the works offering a physical (or mathematical) interpretation of the Nambu, Nambu-Barut, Terazawa, Koide, and other formulas, the problem of elementary particle mass values remains among the unsolved, and one of the key problems of modern physics [3-99]. (Note that listed above are only models of elementary particles' masses, in which the problem of a muon's mass is addressed, either alone or as part of the mass spectrum). The masses of fundamental particles (or proportional to them - (Yukawa) couplings to the Higgs field), including that of muon, are among the free parameters of the Standard Model of elementary particle physics [27,100-102]. In this paper, we present an entirely new model that is not an extension of any existing model.

Note: Not listed, not formally cited, and not discussed in the paper are models (if they represent true models) from preprints (if they can be termed so) hosted on non-institutional repositories, namely, viXra, ResearchGate, and Academia.edu; we, however, choose to mention the existence of such: viXra:2303.0111, viXra:1702.0332, viXra:1611.0142, viXra:2406.0118; DOI: 10.13140/RG.2.2.20983.60323; Saltaoglu, 2024. The same for "preprints" from personal websites, namely, brannenworks.com: Lepton masses as star of David.

Note: Also possible are un-proportional to masses, couplings to the Higgs field outside the Standard Model which is falsifiable (in particular, branching ratio of Higgs boson decay into muon-

antimuon pair is predicted to be 25 times higher than that in the Standard Model due to enhanced coupling) [98].

The main, new idea in the basis of our approach is the assumption that the mechanism of existence of the muon (a 2nd generation elementary particle) is related to the possibility of a 2nd-order structure in the case of interaction of ball-shaped nodes - a structure that, on a smaller scale (from a distance), also looks like a ball (and, presumably, behaves like a ball, i.e., is not destroyed when interacting (contacting) with other similar structures) - and contains a layer of 12 touching one another nodes around the central one, to which they adhere. (The view of 2nd-order ball is novelty, and its application to muon is new, but there are already known examples of 13-ball structures (where the nodes are atoms) that indeed, when interact, only contact (and deform) one another but do not merge (i.e., stay as distinguishable clusters), i.e., behave like 1st-order balls themselves, but on a smaller scale; more details can be found in the 4th section).

The originality of the idea of 2nd-order ball is confirmed by the lack of relevant search results for phrases "second-order ball", etc.

The maximum number of equal-sized balls (or spheres) that can touch the central ball, is dictated by 3D-space, and as 12, was discussed in 1694 by Newton with Gregory, who thought the number should be 13 instead; the first correct proof of number 12 was obtained in 1953 by Shutte and van der Waerden; in our treatment, when ball-nodes falling from infinity (to each other) touch the central node, but before the central node shrinks (a little) to allow shell nodes to touch one another, all ball-nodes are also equal-sized; number 12 is justified also for the structure with the compressed central node since the nodes of a shell only approach each other and get in contact with one another, leaving even less free space in the shell for the incretion of the 13th node [103,104].

In this system of 1 + 12 = 13 nodes, the nodes, or more precisely their centers, are interconnected by 12 + 11 + 10 + ... + 3 + 2 + 1 = 78 bonds (of 4 different types, due to 4 different distances between the centers of different nodes). This formula (for the total number of bonds) is justified by bond-by-bond counting from geometrical representation of the structure, see below. The nodes' (balls') centers around the central node in the structure with the compressed central node and also when this structure is compressed as a whole, are located in the most symmetric way geometrically possible - in a way, quite obviously, closest to the symmetry of a sphere - in the vertices of a regular icosahedron. (The latter is the most spherical Platonic solid, and a sphere possesses the maximal symmetry, as is commonly known; a comparison of the icosahedron with more relevant (than other Platonic solids), non-Platonic polyhedra, is below) [105]. Such an arrangement (icosahedral) is assumed to correspond to the lowest energy state of 13 interacting nodes, so in the model it forms spontaneously. The assumption is grounded by the fact that the most symmetric state and the lowest energy state both are extreme cases, so it is natural to await for them to coincide; the second base of the assumption is the result of simplified case's calculations, where the structure (icosahedral) with the compressed central node was compared with arrangements of ball-nodes in (sequentially) compressed chunks of close-packed lattices, face-centered cubic (FCC) and hexagonal close-packing (HCP) - in which the nodes of a shell are at the vertices not of an icosahedron but of cuboctahedron and triangular orthobicupola, respectively: the icosahedral structure was the lowest in energy; for the third base of the assumption, see the 4th section.

The simplification mentioned is the same as simplifications in tauon's mass calculation, which will be discussed later in this paper. Compared were the bonding energy maxima between the structures; whether these maxima are global was not fully evaluated.

The icosahedron is also calculated to be more spherical than a cuboctahedron and a triangular orthobicupola: the isoperimetric quotient, according to the formula, is 0.83 (icosahedron) and 0.74 (other two solids) - compare with its value for a sphere: 1 [105].

The bonds between the nodes, in the form of forces of their mutual attraction, are assumed by the model to be the simplest possible ones, obeying the law of inverse squares, like gravitation and electromagnetism. Thus, the bonding energy of the nodes is inversely proportional to the square of the distance between the (centers of the) nodes. The mass energy of the 2nd-order structure (muon) is assumed in the model to be the sum of the energy contained in such bonds (interconnection of the nodes) minus the energy spent on the nodes' compression. (Note: considering mass–energy equivalence, the notations "mass-energy" and "energy-mass" will be widely used throughout the paper; such notations in conjunction with discussing the problem of elementary particle masses are used in Kyriakos AG and Kumar N, respectively) [11,18]. Consumption of energy with nodes' compression, as will be shown by calculations below, cannot prevent the structure made of nodes in touch with one another, from contracting to form more tight bonds, but stops the contraction at some point.

The difference between the energies of bonds and of compression of the nodes is equal to the total useful energy, i.e., the energy released to outside of the structure during the bonds' formation: part of the released energy can be treated as going to feed nodes' compression (i.e., is released to inside of the construction). The equality of bonds' energy with the total energy released (to the outside and inside) is obvious since the energy needed to break the formed bond should be equal to the energy discharged during its formation. Only outside part equals muon mass, and is termed *usable* energy; in other words, numerically the same as the outside part is the potential energy of bonds minus the energy that already contracts bonding - i.e., the energy of the nodes' momenta, that is proportional to the degree of the nodes' compression (see details below), which (energy of nodes' momenta) equals kinetic energy if the nodes are assumed massless. Another situation (possibility) - with nodes at rest also should be investigated: a compressed node (e.g., the node in the centre of the construction of 13 nodes) "wants" to decompress (like a spring) - helping one to debond the surrounding nodes because energy releases when the node decompresses: releases

in the form of movement of the node's boundary and thus gives impulse to the surrounding, bound nodes, which makes it easier to take them away from each other; thus, to break the bond, one needs to compensate not all the potential energy, but the part left after the subtraction of energy of nodes' (de)compression; so, the real bonding energy of the nodes is the potential energy of the bonds minus the energy stored in the compressed nodes or energetically equivalently in nodes' momenta.

One can see that both situations include momenta (the nodes are initially in movement, or acquire momenta when the node(s) decompress). But the situations are physically distinct. The difference is that in the second case, the nodes are treated identically to macro-objects or in the context of classical physics or Einstein's relativity where objects can have 0 initial momentum, while in the first case, the nodes' momenta are inherent so the nodes cannot stop, which may imply that they are permeable to each other (to not stop when bouncing from each other, because no bouncing at all); inherent momenta is an attribute of quantum mechanics (e.g., such momenta of electrons create the pressure that prevents white dwarf star from (further) collapse and their (momenta) energy cannot be emitted or somehow taken away, i.e., is not usable).

Let us illustrate the real bonding energy, containing both potential and kinetic energy contributions, also in a macroscopic analogy: bonding energy of two gravitating bodies' system depends on their momenta: if the momenta had been zero, bonding energy would be equal to the potential energy, i.e., of the bodies attraction, which is a function of the distance (between the bodies' centers, according to the Newton's law); the non-zero momenta are subtracted from this (potential) energy, because if the momenta are high enough, the system can become unbound even when the distance between attracting objects is finite. So, it is clear that bonding energy can consists of not only potential energy but (subtracted) kinetic energy as well, as is known for chemical bonds and obvious for bound systems formed by gravitational attraction, perhaps even more clearly—for the comet–Sun system, where potential and kinetic energies reversibly transform into one another, but the bonding energy of the system stays the same [106].

The bonding energy of individual bonds in this paper is calculated with only distances between the nodes (more specifically, between points in the nodes) i.e., potential energy, and only then when summing for the whole structure kinetic component (i.e., energy of nodes' momenta) is subtracted. So, in the rest of the paper, by bonding energy of individual bonds, energy in zero-momentum simplification is given (as in the initial, simplistic treatment of bonds), or potential energy component, i.e., we do not use long term for such bonds: *component of bonding energy that (component) is potential energy,* but use: *bonding energy*. This aids brevity and simplicity.

The bonding energy of a single unbound node, i.e., of a structure of order 1, and thus, as assumed by the model, the mass energy of a free electron, is (unexpectedly) non-zero: instead, it is 4 times less than the maximum binding energy of two nodes, i.e., the binding of them at the minimum distance equal to 1, i.e., the distance when the ball-nodes of radius 0.5 have come into contact and are assumed to be incompressible (incompressibility is a simplification). (Why this simplification, in conjunction with one another (described below), gives the right electron's energy-mass in the sense, that it allows us to compute a muon's mass in units of electron's mass in a good agreement with the experimental value requires further investigation; however, simplification, and even more obviously, the sum of all possible simplifications, cannot lead to the electron's mass-energy to become a free (adjustable) parameter in the model: there is only one way to calculate with the sum of all simplifications.)

Our model does not forbid the possibility of the equality of the theoretical electron's mass with the currently measured one; if such equality is assumed, the theoretical muon's mass in this paper should be viewed as expressed in units of theoretical and experimental masses of electron simultaneously. A choice in favour of the theoretical electron mass can be required in future work: if one wants to predict (not retrodict) the muon's mass, i.e., to go to precision beyond experimental (see details later in this paper).

The ratio of binding energies (1:4) can be justified by the sequence of square numbers $1^2 = 1;2^2 = 4;3^2 = 9$, which is non-arbitrary, and which part (4,9) is reproduced from physical-geometrical considerations in Figure 1 i.e., one can see that if the bond energy of two nodes corresponds to 4 units of energy, the cumulative bond energy of three nodes arranged in a most simple way 1D (i.e., in a line) is 9; then, in continuation of the sequence, the energy attributed to an individual node is 1.

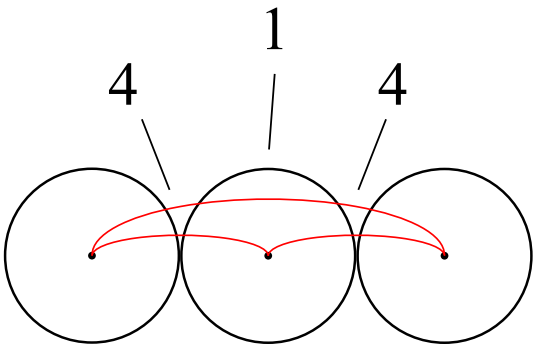

Figure 1: Maximal bonding energies of two and three ball-nodes arranged in a row (nodes are represented by circles that are their slices or equivalently projections); the numbers are the energies of individual bonds (of pairs of nodes); the maximum bonding energy of two nodes is 4, not 1; please, sum in mind 4 + 4 + 1 to obtain the maximal bonding energy of three nodes; bonds between every two nodes (inversely proportional to the square of the distance) are calculated assuming (simplifying) the interaction of node centers only (e.g., if the entire density is concentrated in the centre of a node) and ball-nodes' incompressibility

Relation 4:9, which can be seen in the Figure 1 is derived (in details) as follows: calculating the bonding energy of two nodes at distance 1 gives $1/(1^2) = 1$, where 1 in brackets is the distance, and analogously, the binding energy of three nodes is $[1/(1^2) = 1] + [1/(1^2) = 1] + [1/(2^2) = 0.25] = 2.25$; the relation between the two energies, 1:2.25, can also be expressed as 4:9 - from which the bonding energy of one node is extrapolated (i.e., of a free node, so the physical meaning of bonding energy in this case (apart from it as the energy of an electron) awaits for interpretation).

In addition to positive energy, i.e., bonds' energy (termed "positive" at least since it adds up to muon's mass), negative energy is introduced into the model since, as mentioned above, energy is absorbed in the contraction of individual ball-nodes (this energy is subtracted from the muon's mass). (Herewith, note that the contraction of the entire construction of 13 nodes, as a result of the contraction of individual nodes, can proceed both with the cumulative release or consumption of energy, i.e., spontaneously or not, respectively, which depends on the considered scale of the structure, amount of contraction). During contraction of the structure with the nodes already just in contact with one another (shell nodes with one another and with the (compressed) central node), which we take (conditionally) as initial, uncompressed structure, starting point for calculations, it is possible both (further) compression of the central node-ball in three directions (along three coordinate axes) and flattening of the nodes of the outer layer along the direction to the centre of the structure (depending on the degree of this flattening, the central node can undergo not only compression but (relative) relaxation). The structure's compression "at first steps" results in the cumulative release of energy, but when the rate of energy release due to bringing the nodes closer together equals the rate of energy absorption from compressing the nodes, or, equivalently, when the forces of attraction and repulsion reach equilibrium at some point, the structure will cease to spontaneously contract. The repulsive force is thought to be of a quantum-mechanical nature and is represented by an equation that is similar to the Heisenberg uncertainty relation:

$$dd_1 d_2 p=1, \qquad (1)$$

where d, d_1, and d_2 represent the diameters of the node in three mutually perpendicular directions, e.g., along the x, y, and z coordinate axes, respectively; p denotes the momentum equal to the energy absorbed during compression of the node, in sum with the energy of the initial momentum taken as 1 in the model (why this value does not cause an (unsolvable) problem because being equal (but with the opposite sign) to the maximal bonding energy, see below); the latter (initial momentum) is the momentum when all the aforementioned diameters = 1. Momentum here is equal (and equivalent) to energy (absorbed in compression of the node) since the well-known relativistic energy– momentum relation $E= [(pc)^2+ (m_0 c^2)^2]^{1/2}$ (where c is the speed of light and m0 is the rest mass), if written in natural units ($c = 1$), reduces to $E = (p^2 + m_0^2)^{1/2}$, which, if the nodes are assumed massless, further reduces to $E = p$.

The energy of the initial momentum (=1), when summed of two contacting nodes (1 + 1 = 2), is higher than their maximal bonding energy (= 1), so, when subtracted from the latter, gives an unbound system, which poses a problem. The possible solution comes from interpreting the ball-nodes as solitons (i.e., nonlinear, particle-like waves, the first sort of which was observed in 1834 by Russell, and many other kinds were discovered and studied later) [107]. Both solitons and other (linear and nonlinear) waves must move to exist, so they have non-zero intrinsic momentum [108]. Among them, solitons (as was said) are particle-like and can (theoretically) have ball shape, thus making them suitable to describe ball-nodes (however, some kinds of solitons, if ball-shaped, are unstable) [109,110]. Imagine the firstly-observed soliton, that of Russell, described by him as a moving, "round, smooth and clear water hill"; now imagine two such hills moving in the same direction (so they are at rest relative to each other): their momenta obviously do not contract their (imaginable) mutual attraction, i.e., do not cause any repulsive force (because momenta are 0 in the frame of both solitons); analogy can be applied to the ball-nodes (two or 13), so their intrinsic momenta, or more specifically initial intrinsic momenta, should not be counted when computing bonding energy of the whole (13-ball)

structure (muon) [107].

The momenta directed in opposite directions (and thus non-zero in the frame of two interacting objects) are assumed to emerge only when one tries to push solitons to be superposed on each other, which instead forces them to deform (flatten) and gives the opposite momenta: the higher the push, the higher the momenta. The assumption is grounded by the fact that solitons are shown, by calculations, to bounce each other (in contrast to linear waves (e.g., sound waves) that freely pass through each other thus one can hear all instruments in orchestra), which imply impermeability and thus may imply flattening during interaction (including - collision) [111]. Solitons are also observed and calculated to have finite length, so they are not superposed on each other when their centers are far enough, which also grounds the assumption (however, finite length (computed) may be due to limitations of the models applied; the question of justification of the finiteness of ball-node in our model is discussed, mostly, in the 4th section) [111].

Another to Eq. (1), possibility, is also considered: initial momentum is 0 but the rest mass equals 1 (i.e., the nodes are assumed not massless); in this case, p in Eq. (1) should be replaced with m, which is the relativistic mass also equal E, due to mass-energy equivalence: $E = mc^2$ reduced to $E = m$ when c is in natural units. Note that the relativistic mass also implies nodes' movement, however, only in the compressed structure's case (not counting the central node, which is already compressed); the (possibility of) aforementioned variant where the nodes are not moving even when compressed will be discussed later in this work. Question of choosing between the two non-stationary nodes' variants above will be treated later in this paper. The initial 0 momentum variant is trivial, as was said - if considering classical or macroscopic objects or Einstein's relativity; but the non-zero (= 1) value of initial momentum also can be justified in addition to the aforementioned arguments by analogy of (1) with Heisenberg's formula ($\delta_x \delta_p \geq$ constant), in which for every component of the formula (i.e., δ_x (position uncertainty), δ_p (uncertainty in momentum), and the constant), it is forbidden to be zero; we then choose the simplest non-zero values, i.e., 1 (or it can also be −1) for every variable in (1), thus the built-in non-zero values of p, d, d_1, and d_2 are justified in our model as the simplest, so they can't be an adjustments, i.e., free parameters.

Also in the Heisenberg relation, it is valid (both physically and for convenience) to choose units in which the constant is expressed as equal 1 (called *natural units*); if values of both δ_x and δ_p also equal 1, this comprises one of the valid solutions; in that case, the only difference between the two formulas (apart from ≥ and = signs) is that in ours, not uncertainty of momentum but momentum itself is considered, and not uncertainty of position but ranges of positions (on coordinate axes)—diameters are used [107]. Furthermore, the minimum uncertainty of momentum can be taken as the momentum; the minimum uncertainty in momentum is if instead of the ≥ sign, the = sign is placed in Heisenberg's formula as in (1) [112]. (Further justification and explanation of the parallel with the Heisenberg formula is out of scope of this paper and can be addressed, e.g., to an interested reader).

The repulsive force in the model is assumed to be of the same nature as the attractive force (i.e., they are different manifestations of one force and thus have the same interaction constant). Thus, attraction, which is inversely proportional to the square of the distance, disappears at distance 1, and at distance < 1 it changes to repulsion (described by (1), i.e., at first it is small but grows with decreasing ball's diameter). (Note that the repulsive force is not between the points but due to inevitably accompanying the distance < 1, ball-node's compression.) I.e., the repulsive force occurs when the node starts to deform (shrink) to a diameter < 1 at least in one direction, or equivalently the distance between the centers of nodes becomes < 1. Thus, considering the attraction between nodes' centers only (that are, e.g., centers of mass), two nodes at distance 1 stop (thus avoiding the emergence of repulsive force, which requires energy consumption) if they are not under pressure from neighbouring nodes (at that distance, they both have diameter 1). However, in the construction of 13 nodes, there are still nodes at distances > 1, which still benefit from further approaching each other and, as a consequence, put pressure on their neighbours, in particular on the central node, and the structure of the contacted balls undergoes further spontaneous collapse, as noted, to the equilibrium of forces and, at the same time, to the maximum of the released useful energy (i.e., to the lowest energy state).

In the positive energy (i.e., energy of bonds) calculation, the model further considers the distance between two nodes not as a distance between nodes' centers only (which was a "first step", i.e., simplification) but as the distance between two points located with a certain probability at some distance from the center of each node. Each node thus turns into a ball filled with points, each of which represents one of the possible positions of the node as a point (classical) particle (the ball in this case can be viewed as no longer representing a node but a boundary of point nodes' distribution; for simplicity, we continue to use ball-node notation through the paper) or, alternatively, it is a node's center (which implies uncertainty in the position of the whole ball-node); also, there may be many (noninteracting with each other) points co-existing in the ball-node (comparing this and other possibilities is out of the scope of this work). The distribution of points within the ball node is assumed to be somewhat analogous to the possible positions of an electron on the s-orbital in an atom, i.e., as a concentration of points toward the center (along the x, y, and z axes) [113].

However, rather than being described in terms of quantum mechanics, the delocalization of the node as a point is modelled classically in this work: the probability of finding a point is inversely proportional to the cube of the distance from the node's center (the view on the origin of such a dependence can be found in section 4). The probability is distributed only within each ball-node of diameter 1, i.e., the chance of encountering a point outside a ball of diameter 1 equals zero (the argument for this assumption is that 1 can be considered the size of the soliton; further justification is in the 4th section).

2. Method

The computations were performed using the 32-bit Windows (Microsoft Corp) standard calculator. The calculation of

distances between points within the ball-nodes was carried out using random numbers as coordinates of points. The random numbers were obtained using the π sequence (i.e., extracted from it) in a way that enables the possibility of independent verification of the outcomes: The sequence of actions (algorithm) is as follows: For the first calculation (first iteration), we discard "3." from the number π and use the first 10 integers to determine the coordinate of the point on the x-axis in the first ball by adding "0" before these integers, so we have: $x = 0.1415926535$ [114].

According to the sphere formula for a sphere centred at the origin of coordinates,

$$x^2 + y^2 + z^2 = R^2, \qquad (2)$$

where x, y, and z are the point's coordinates, and R is the sphere's (or ball's) radius.

If x is given and $R = 0.5$, then the value of the left side of equation (3) is known.

$$y^2 + z^2 = R^2 - x^2. \qquad (3)$$

The next random number, obtained by the method described above, will denote the fraction (uniformly distributed from 0 to 1) that y^2 has from the left or, numerically, the same, right, part of equation (3), i.e., from y^2+z^2 or R^2-x^2. Let's call this number p, from "part" (not to be confused with momentum p).

$$y^2 = p(R^2 - x^2); \qquad (4)$$

$p = 0.8979323846$.

Then z^2 represents the remainder:

$$z^2 = R^2 - x^2 - p(R^2 - x^2). \qquad (5)$$

Then we take from the π sequence the coordinate and fraction for the neighbouring ball:

$x_1 = 0.2643383279$,
$p_1 = 0.5028841971$.

Thus, as of now, two points on the surface of two balls are defined. Then, these points must be able to exist inside the ball-nodes, within their volume. For this purpose, each coordinate (x, y, z) is multiplied by the same random number from 0 to 1 (and each coordinate x_1, y_1, and z_1 by the same another number also from 0 to 1). Through this action, the scale of the sphere is reduced, making it a "spherical slice" of the ball. We obtain these numbers in the way noted above from the further sequence of the number π for each of the connected ball-nodes, respectively:

$c = 0.6939937510$,
$c_1 = 0.5820974944$.

In order for the points (and spherical slices of the ball) to concentrate toward the center of the ball-nodes, the numbers c and c_1 in the calculation process (below), as implied by the modelled cubic dependence noted above, are additionally raised to the cube. Let us calculate the distance between the random point within a shell node and the random point in the central node: type 1 distance. The positions of the nodes are shown in figure 2. The center of the central node coincides with the center of every one of the three golden rectangles located at right angles to each other in the icosahedron, see figure 3. The centers of shell nodes (including those on figure 2) coincide with the corners of such rectangles, so they can be viewed as white points on the edges of the rectangles in figure 3.

The distance between random points in the two balls (central and that of a shell) along the x-axis is:

$$rk - 0.5ftxc^3 + t_1x_1c_1^3(rk - 0.5f), \qquad (6)$$

where rk, or r itself if $k = 1$, is the radius of the circumscribed sphere around the icosahedron; rk or, when $k = 1$, r, is equal to the distance between the centers of the nodes under consideration (from the relation for a (regular) icosahedron, $r = \frac{a}{4}(10 + 2\sqrt{5})^{1/2}$, where a is the length of the icosahedron's edge; taking $a = 1$, we have r as a number starting with 0.951, with 32 decimal places intended for use in the aforementioned 32-bit Windows calculator; the number can be found in Supplement 1); f is the affine transformation of the x coordinate, i.e., describes the degree of flattening of the shell node (on figure 2, non-dashed) along the x-axis (node flattens if $f < 1$): multiplication of the x-coordinate of a random point by $f < 1$ decreases its position along the x-axis toward 0; k is the (calculable) parameter that does not equal 1 only in the case of $f < 1$, and will be discussed later in this section; multiplication by 0.5 is due to the fact that the radius and, respectively, the scale of the considered ball node is 0.5; t and t_1 are numbers taking values 1 or −1, given that (random) coordinates should be able to have both "+" and "–" signs: if the last number in x or $x_1 = 0$, 1, 2, 3, or 4, we choose the sign "–" (and thus replace t or t_1, respectively, with −1); if 5, 6, 7, 8, or 9, we choose "+" (and thus delete t or t_1, respectively, which is equivalent to replacing them with 1); ($rk - 0.5f$) is the radius of the central node of the construction, linked to the radius of the shell node along the x-axis (the latter is 0.5f); x_1 (of the random point in the central node) here has the meaning not of a coordinate but of an addition to rk (i.e., to the distance between nodes' centers along the x-axis; depending on the sign of t_1, the addition can be positive or negative); (x_1 would be the meaning of a coordinate if the origin were located at the center of the central node, which is not the case in figure 2) [115].

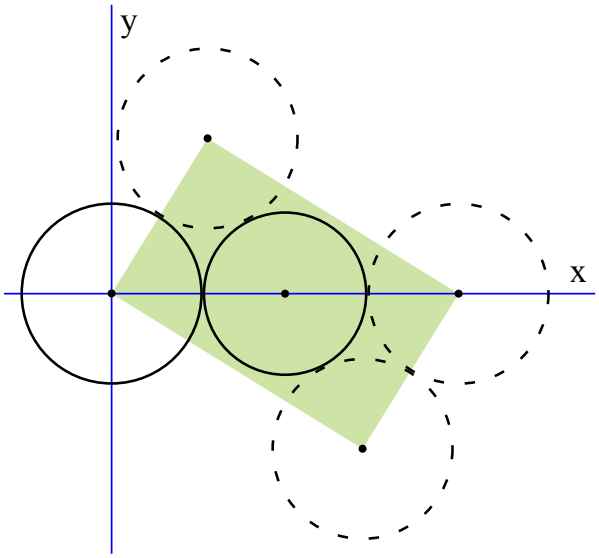

Figure 2: The central node of the construction (right, non-dashed), compressed to the size corresponding to the mutual contact of the shell nodes nearest to each other; shell nodes here are all dashed circles and left non-dashed one (more precisely, on the figure are shown nodes' projections, or equivalently, slices in the widest parts of the nodes); also shown is the location of the nodes in relation to the so-called golden rectangle, inscribed in the icosahedron (all slices (projections) of the nodes lie in the plane of this rectangle)

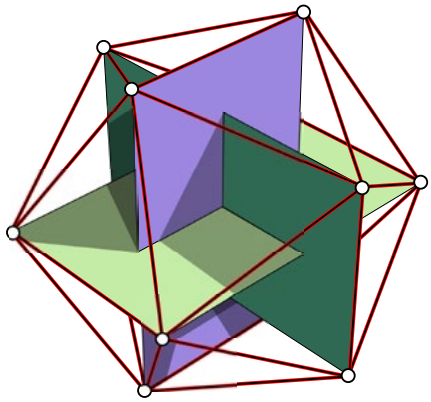

Figure 3: Three orthogonal rectangles are inscribed in a regular icosahedron (image by Fropuff, Mysid, public domain, via Wikimedia Commons)

The *y*-axis distance between random points of the nodes in consideration, accounting for (4) and that the affine transformation of the *x* coordinate does not affect the *y* and *z* coordinates (thus, *f* is not used in describing *y*), is:

$$y - y_1 = t_2(p\{[0.5c^3]^2 - [0.5xc^3]^2\})^{1/2} - t_3(p_1\{[c_1^3(rk - 0.5f)]^2 - [x_1c_1^3(rk - 0.5f)]^2\})^{1/2}, \quad (7)$$

where by variables t_2 and t_3 is taken into account that square roots can be both positive and negative numbers (or, in other words, random *y* and y_1 can be both positive and negative as a result of multiplication by t_2 or t_3); the choice of "+" and "–" is made according to the rule noted above, but based on the last digits in the numbers *p* and p_1, respectively; "*rk*−0.5*f*" is the aforementioned radius of the central node.

Distance along the *z*-axis, given (5):

$$z - z_1 = t_4(\{0.5c^3\}^2 - \{0.5xc^3\}^2 - p\{[0.5c^3]^2 - [0.5xc^3]^2\})^{1/2} - t_5(\{c_1^3[rk - 0.5f]\}^2 - \{x_1c_1^3[rk - 0.5f]\}^2 - p_1\{[c_1^3(rk - 0.5f)]^2 - [x_1c_1^3(rk - 0.5f)]^2\})^{1/2}, \quad (8)$$

where the variables t_4 and t_5 are to be replaced by −1 or 1 according to the above-mentioned rule, but based on the last numbers in *c* and c_1, respectively.

In total, the distance l_1, between random points in two balls, the central ball and any node of the shell, squared (squaring is a preparation step for using the distance in the computation of bond energy: as noted above, it is inversely proportional to the square of the distance), i.e., type 1 distance squared, is the sum of squared (6), (7) and (8), i.e., the sum of squares of distances

along *x, y*, and *z* axes. The formula (of distance l_1^2) can be found in Supplement 1. Let us compute the distance between a random point of a shell node and a point within the nearest node, also located in the shell - the distance of type 2: The arrangement of the nodes is shown in figure 4.

When calculating the distance, we rotate counter-clockwise around the origin at the center of the construction (that is, simultaneously, the center of the central node, point A on figure 4), one of the nodes initially (not physically, but during the calculation) superimposed on each other; the original x' and y' coordinates belonging to the node rotated around A will thus become the new x'' and y'' coordinates:

$$x'' = x' \cos g - y' \sin g, \qquad (9)$$

$$y'' = y' \cos g + x' \sin g, \qquad (10)$$

where g is the rotation angle (here it is positive because the direction of rotation is counter-clockwise, the positive sign is according to convention); from the relations for an icosahedron, g's rounded off value is 63.435 deg (in computations is used this rounded value for the reasons that can be found in the 5th section). (Angle derivation: the distance from the center of the rectangle (point A on figure 4) to the corner of such a rectangle (and thus to the center of the node of the shell), as noted above, $= \frac{a}{4}(10+2\sqrt{5})^{1/2}$, where a is the length of a small side of such a rectangle (and at the same time, of an edge of the icosahedron on figure 3); in right triangle formed by the first distance as hypotenuse and half of the second distance as cathetus, the angle at the vertex at point A is $\sin^{-1}[\frac{a}{4}(10+2\sqrt{5})^{1/2}/(0.5a)] =$ 31.717474411461005324213903139774 *deg*; double the value of the latter is the sought-for angle before rounding.)

Herewith,

$$x' = rk + 0.5ftxc^3, \qquad (11)$$

because initially, the rotated node was located at the place of the lower node in figure 4, the center of which lies on the *x*-axis; in this calculation, *x* has the meaning of the value of the addition to the $x''' = rk$ coordinate, not the value of the *x*-axis coordinate itself (i.e., $x''' + x(0.5ftc^3) = x'$, which (x') after node's rotation will turn to the final *x*-coordinate of a point: x'').

$$y' = t_2\{p[(0.5c^3)^2 - (0.5xc^3)^2]\}^{1/2} \qquad (12)$$

Substituting to (9) and (10), respectively:

$$x'' = \{rk + 0.5ftxc^3\} \cos g - t_2\{p[(0.5c^3)^2 - (0.5xc^3)^2]\}^{1/2} \sin g, \qquad (13)$$

$$y'' = t_2\{p[(0.5c^3)^2 - (0.5xc^3)^2]\}^{1/2} \cos g + \{rk + 0.5ftxc^3\} \sin g. \qquad (14)$$

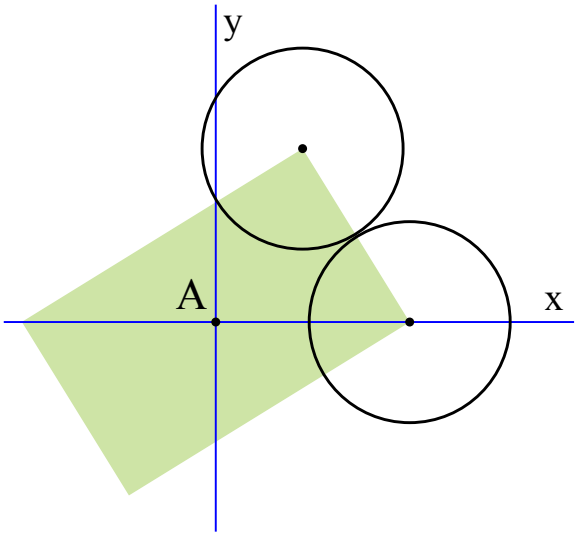

Figure 4: Location of a shell nodes closest to each other, in relation to the center of the central ball node (A) - the node is not shown, and to one of the (mutually perpendicular) rectangles in the structure

Distance along the x-axis (between two points in two nodes), given that, similar to the case x',

$$x_1' = rk + 0.5ft_1x_1c_1^3, \qquad (15)$$

is

$$x'' - x_1' = \{rk + 0.5ftxc^3\} \cos g - t_2\{p[(0.5c^3)^2 - (0.5xc^3)^2]\}^{1/2} \sin g - \{rk + 0.5ft_1x_1c_1^3\}. \qquad (16)$$

Distance along the *y*-axis:

$$y'' - y_1 = t_2\{p[(0.5c^3)^2 - (0.5xc^3)^2]\}^{1/2} \cos g + \{rk + 0.5ftxc^3\} \sin g - t_3\{p_1[(0.5c_1^3)^2 - (0.5x_1c_1^3)^2]\}^{1/2}. \qquad (17)$$

Distance along the z-axis (which is not affected by the rotation of the first node):

$$z - z_1 = t_4\{[0.5c^3]^2 - [0.5xc^3]^2 - p[(0.5c^3)^2 - (0.5xc^3)^2]\}^{1/2} - t_5\{[0.5c_1^3]^2 - [0.5x_1c_1^3]^2 - p_1[(0.5c_1^3)^2 - (0.5x_1c_1^3)^2]\}^{1/2}. \quad (18)$$

In total, the distance l_2, between the points in the two closest nodes of the shell, squared (type 2 distance squared), is the sum of squares of (16), (17), and (18), and is written in Supplement 1. Let us calculate the distance l_3, between a random point of a shell node and a point within the second in proximity, a shell node, i.e., the type 3 distance: The arrangement of the nodes is shown in figure 5. The centers of the nodes, as seen, are at the ends of the larger side of one (it can be any) of the rectangles in figure 3. The formula is the same as for the type 2 distance case, except that it contains the rotation angle j instead of g, which (*j*) is ≈ 180 − 63.435 = 116.565 deg (this approximation is used in calculations and is only due to 63.435 is the rounded number). The formula describing the distance l_3 squared is in Supplement 1.

Let us calculate the last type of distance, l_4, between a random point within a shell node and a random point within the third in proximity, i.e., the farthest shell node, the type 4 distance: Positions of the nodes are shown in figure 6.

Distance on the *x*-axis:

$$2rk\text{-}0.5ftxc^3 + 0.5ft_1\, x_1\, c_1^3 \quad (19)$$

where x and x_1 are used as values of additions (which can be negative, depending on t and t_1) to the distance between nodes' centers.

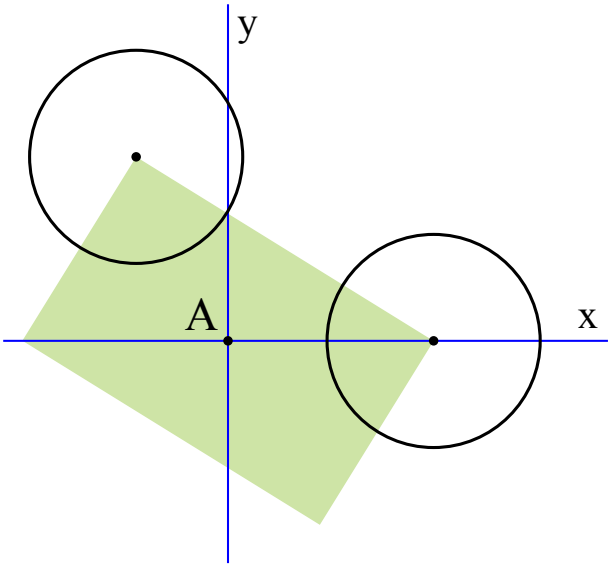

Figure 5: Location of two shell nodes, second in proximity to each other; point A is the center of the construction; green is one of the golden rectangles in the latter

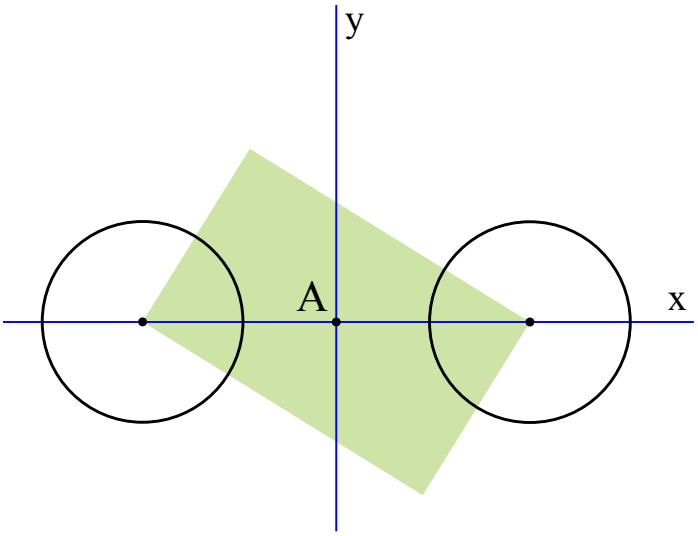

Figure 6: Location of two most distant from one another, nodes of the shell, relative to one another and to the center of the central node (A) - the node is not shown, and to one of the rectangles inscribed in the icosahedron

Distance on the y-axis:

$$y - y_1 = t_2\{p[(0.5c^3)^2 - (0.5xc^3)^2]\}^{1/2} - t_3\{p_1[(0.5c_1^3)^2 - (0.5x_1c_1^3)^2]\}^{1/2}. \quad (20)$$

Distance on the *z*-axis is the same as for the nodes on figures 4 and 5, i.e., (18). The squares of the distances along the *x, y*, and *z* axes altogether give l_4^2 (type 4 distance squared), which is placed in Supplement 1. Now let us figure out the bonds' energies, i.e., the positive energy, for each of the 4 cases:

The sum of binding energies for distances of type 1, termed (the sum) E_1, is

$$[1/(l_1^2)] \times 12 \times 4, \quad (21)$$

where l_1 is the distance of type 1; 12 is the number of distances (or bonds) of this type in the structure (that number can be seen with the aid of figure 3 as all distances from the center of the central node to the centers of the shell nodes), 4 is the coefficient of conversion of energy into electron masses justified above (in conjunction with figure 1), and 1 in the numerator can be viewed as a constant (or further interpreted as the nodes' or points' mass (in analogy with Newton's law of gravity, so it actually comes from 1^2), but this mass does not add to muon mass because the latter is calculated (or assumed), simply speaking, as bonding energy and not the energy (mass) of points (nodes) that are bonded; in details mass of muon is computed as real bonding energy (i.e., after subtraction of node momentums or equivalently, relativistic adding's to initial node masses) without the initial energy (mass) of points/nodes). (Further considerations of why the energy-mass of a node (point) does not add to the muon's mass can be found in the 4th section).

The sum of binding energies for type 2 distances (or bonds), E_2, equals, analogously:

$$[1/(l_2^2)] \times 30 \times 4, \quad (22)$$

where l_2 is the distance of type 2, and 30 is the number of bonds of this type in the construction (this number equals the number of edges of the icosahedron (figure 3), which are the distances between the centers of the closest shell nodes, see figure 4).

The total binding energy for type 3 distances, E_3, is

$$[1/(l_3^2)] \times 30 \times 4, \quad (23)$$

where l_3 is the type 3 distance, and 30 is the number of bonds of this type in the structure (to obtain that number, choose any pentagon on figure 3, which is the base of a pentagonal pyramid; in the pentagon, you can see that one of the distances between nodes' centers coincides with the larger side of the rectangle, it is l_3 (see figure 5); from symmetry considerations, it can be seen that there are 4 more equivalent to l_3, distances in the pentagon; so, in total, there are 5 l3's in the basis of the pentagonal pyramid; on the opposite side of the icosahedron there should be an analogous pyramid, which adds 5 more l_3's; next, there are 10 faces that form a belt between those pyramids, and accounting that type 3 distance is between the farthest points of two adjacent faces, one can see, using figure 3, 10 more l_3's in the belt; the next 5 l_3's are the distances between the top point of the pentagonal pyramid considered at the beginning and the most distant points in faces in the belt, that are adjacent to every face containing the top point; the last 5 distances of type 3 are seen in the same way but with the pyramid on the opposite side of icosahedron).

For distances of type 4, the bonding energies' sum, *E*4, is equal to

$$[1/(l_4^2)] \times 6 \times 4, \quad (24)$$

where l_4 is the distance of type 4, and 6 is the number of bonds of this type in the construction (these are diagonals of golden rectangles; there are 2 such diagonals in every rectangle, so 6 in total; from figure 3, one can see that every shell node participates in forming one of those diagonals, which can be seen as distances between the tops of two pentagonal pyramids on the opposite sides of the icosahedron, so every shell node can participate only in one of such distances, thus justifying that there are only 6 bonds of this type).

When changing (decreasing) the scale of the construction and calculating (changing due to this) bond energies, the calculated distances (l_1–l_4) are multiplied by the same scale factor *s* (*s* < 1); practically, multiplication takes place after extracting square roots from l_1^2 - l_4^2 (details are below).

The negative energy is calculated as follows: As mentioned above, when the node-ball's diameter (*d*) equals 1, it is assigned a momentum of 1, so when the momentum is multiplied by the diameter (or diameters in each of the three directions, along *x, y,* and *z* axes, i.e., *d*, d_1, and d_2, respectively), it equals 1, which is a constant (as in the Heisenberg uncertainty relation); substituting into (1), we have:

$$p\ (= 1) \times d\ (= 1) \times d_1\ (= 1) \times d_2\ (= 1) = 1. \quad (25)$$

In the case of node-ball's compression, the momentum must increase for the outcome to equal 1 (constant). For example, *p* becomes = 4 when the node flattens to the diameter along *x* (from = 1) to = 0.25:

$$p\ (= 4) \times d\ (= 0.25) = 1. \quad (26)$$

It can be noticed an analogy with the Lorentz–FitzGerald contraction (i.e., length contraction) of an object when its speed and accordingly, momentum, increase; obviously, there should be at least a connection between (26), describing flattening of an object (here the node) if its momentum grows, and the theory describing the length contraction (i.e., special relativity); in both special relativity and (1), *p* goes to infinity if length, *L*, which = *d* if in a ball and measured in the direction of movement, goes to zero (so, it is clear that the theories converge to each other at least in the limit).

Note: In doubly special relativity (DSR) theories (which extend special relativity), both p and L are postulated to have their limits (analogous to c is a limit of speed); if DSR is true, our statement should incorporate instead: p goes to its upper limit (equal to Planck energy, E_P), while L, = d, goes to its lower limit (the minimum possible length, Planck length (L_P), linked with E_P as $L_P = 1/E_P$); the DSR idea is falsifiable, [116].

In other cases, values of p calculated from special relativity and (1) diverge at least since initial p is 0 and 1, respectively. But as was explained in the 1st section, (1) is only one (the first) of (at least) two possibilities assumed by our model; another is:

$$dd_1d_2m=1, \qquad (27)$$

where m is the relativistic mass. We claim that the length–mass dependence in special relativity and according to (27) are equivalent to each other (i.e., converge to each other not only in the limit case but everywhere).

Proof: It is shown, from combining formulas of special relativity ($m = m_0/(1 - v^2/c^2)^{1/2}$ and $L = L_0(1 - v^2/c^2)^{1/2}$), that $mL = m_0L_0$ = constant, where m and m_0 are mass of a moving object and its rest mass, respectively; L and L_0 are length of that moving object and its initial length (i.e., at rest), respectively; so one of the possible solutions is [117]: m (= 4) × L (= 0.25) = m_0(= 1) × L_0(= 1) = constant (= 1) (in natural units). Values 4 and 0.25 are one of the possible, dictated by m_0 and L_0, e.g., they cannot be, in pair, 3 and 0.1, respectively; all valid solutions (i.e., pairs of numbers, which, multiplied on each other, give 1) form a half of an upper half of a hyperbola (xy = 1) i.e., the half, that is restricted to positive numbers (coordinates) and further restricted to be the half that depicts x decreasing from 1 to 0 (as L or d do), and y growing from 1 to ∞ (as m do), and not the opposite (i.e., e.g., not L growth); visualizations of the hyperbola for xy = 1 case can be easily found on the Internet. A relationship of the same form can be obtained from (27):

$$m\ (=4) \times d\ (=0.25) = m'(=1) \times d'(=1) = \text{constant}(=1), \qquad (28)$$

where m' and d' are initial relativistic mass and initial diameter (i.e., both-before compression of the node).

All possible solutions to (27), part of which (i.e., solutions) is depicted in (28), form the same quarter of the hyperbola. So (accounting $L = d$), the claim is proven (for 1D-case (object's contraction only in length), which special relativity describes). Although maybe redundant, it can be further verified by calculation through the velocity of an object: using the length contraction calculator on the Hyper Physics website (hosted by Georgia State University, Atlanta, GA 30302), one can quickly obtain an object's velocity (v) that corresponds to 0.5 contraction of its initial length ($v = 0.866c$, where c is the speed of light); substituting this velocity to the well-known and noted above formula for relativistic mass (m), one can compute that such a velocity and thus 0.5 length contraction, correspond to ×2 growth of mass (up to rounding error). Analogously, one can check that the velocity giving a 0.25 length contraction corresponds to ×4 rise. All these numbers are in line with calculated from (27), including in (28); (note: two of the three diameters of an object do not represent length and stay = 1, thus not entering the calculation).

So (27) is now the variant (in negative energy calculation), justified (for 1D case) by established physical theory (special relativity). Another variant, (1), is also justified (as was previously shown), by analogy with quantum uncertainty formula (which is, by the way, also 1D) plus through $p = E$ (where p is for massless object in special relativity, such p can be termed also $p_{massless}$) and $m = E$, which leads to $p_{massless} = E = m$ and thus m can always be substituted by p of massless object (i.e., there is a correspondence); thus, special relativity also justifies (1). In sum, variant (1) has advantage of being in line with both special relativity and quantum mechanics (QM); from perspective of QM (more specifically analogy with Heisenberg's formula), (1) seems applicable to quantum objects, to which the nodes are at least close (can be interpreted as sub-quantum or sub-elementary level); but the variant (27) has advantage of justifying the value of numerator in bonds' potential energies' calculation, see (21) and the description of the latter; however, this numerator (= 1) can be also justified as the simplest whole number which allows (in contrast to 0) to compute bonding energy. In summary, we cannot choose between (1) and (27) but the choice, if will be possible in the future, will not affect numerical results since both variants are numerically the same (for E), and can be viewed as different interpretations of a more general, "length-energy" expression:

$$d\,d_1d_2E=1. \qquad (29)$$

The difference is only that the energy (E) if using (1), is interpreted (as was mentioned) as purely kinetic, while in (27) it is the sum of kinetic and potential energies, where potential is the energy stored in the non-zero m_0; for consistency, third possibility (or interpretation) can be added: no kinetic energy, the energy is only potential: in such a case the nodes are deformed (including, flattened) not by means of movement (implied by momentum or relativistic mass) but by action of a force (field) that links the nodes; the nodes assumed not able to freely move through one another (which is true (were observed) for elementary particles, and solitons); this, third interpretation of (29), is the easiest way to visualize (in mind) our construction as a whole, while the first two variants imply dynamics: many constantly changing to one another configurations equal in bonding energy (in (visual) analogy with many possible states of Sun–comet system or of a globular star cluster). Not moving (termed *stationary*) objects, not depending on their composition, can indeed, according to established physics, or more precisely general relativity, deform (length contract) if placed in fields [118]. Such effects, however, are likely not yet checked observationally (except for photons in the context of gravitational redshift) and are not to be confused with observables like the flattening of a ball filled with water on the Earth surface, which is through another mechanism: molecules' rearrangement; (visual) similarity and identical cause (field), however, deserves to be explained or investigated, and all theoretical cases where the stationary nodes flatten in a field not due to the length contraction, or in sum with length contraction, even can be considered; however, details on the latter cases are

out of our scope in this paper [119,120]. Overall, obtaining the justification of the third interpretation by finding that the variant is possible with established physical theories seems to involve classical physics or it plus general relativity (for the cases out of the scope) or general relativity (of Einstein).

To be more concrete in our assumption of general relativity involvement, we report here that the theoretical tauon's mass in simplified model (that will be discussed in more details in the 4th section), i.e., the minimum energy state, is obtained when all (20 types of) distances between the nodes' centers become 0.5 of the initial ones (i.e., the factor $s = 0.5$, with uncompressed ($s = 1$) structure taken as when the minimal initial distance equals 1, not 0.951 as in the muon's case: so, the inner layer's nodes ($d = 1$) in tau initially do not touch one another, but the central node ($d = 1$), while in muon, respective nodes ($d = 1$) touch one another, which require the central node to be (slightly, to $d = 0.90$) compressed; so s's in muon's and tauon's models are not precisely comparable); one possible (and, presumably, simplified) interpretation of this ($s = 0.5$) final state is that all the nodes shrink to 0.5 (exact number) in all their (three orthogonal) diameters; one of the diameters can be viewed as length, so the 0.5 length contraction is included; such a value of length contraction of an object is achieved also in the vicinity of a black hole, at a distance of $\frac{4}{3}\ R_S$ where R_S is the Schwarzschild radius (these values: of 0.5 length contraction and $\frac{4}{3}\ R_S$ (the latter in the form of $1.33R_S$, which is approximate) are computed in the frame of general relativity); assuming analogy, one can estimate how strong the field that links the nodes in tau-lepton is (or should be) i.e., comparable to strong gravity near a black hole and conclude (preliminary) that general relativity is applicable to describe and/or explain stationary nodes' shrinkage (and thus the value of negative energy) in tau-lepton and so also in muon (accounting that length contraction in gravitational field takes place in the radial direction, i.e., like in flattening of the nodes) [118,121].

From symmetry considerations, an object fallen to the center of gravity cannot be flattened (i.e., only length contracted) but instead should be equally contracted in all dimensions (that is true for the central node in a muon). Is it possible in gravitational field, with general relativity? If a gravitating object, e.g., the Sun, is simplified to have a uniform density, its interior can be (mathematically) divided without remainder into smaller and smaller balls that are placed in free space between bigger and bigger ones; the biggest can be, e.g., 6 balls in pairs along x, y, and z axes, around the center; each such ball (either a small or big one) has a corresponding R_S less than 2.9 km (i.e., less than that of the whole Sun), and can be simplistically treated as a point source of gravity; now imagine a probe object, placed into the center of the Sun, between all the balls: it gets length-contracted in the direction of the ball (one of the biggest) that lies on the x-axis, to the extent described by the factor obtained with general relativity: $[1 - (R_S/R)]^{1/2}$, where R is the distance to the center of that ball (in units of R_S; equivalently, R_S and R can be in km); but at the same time, the probe object gets length contracted in a direction to the analogous ball on the y-axis, i.e., in the perpendicular direction, and to the same extent; the same is true for the z-axis [118,122]. So, in total, a probe object is length-contracted (if it can be said so) in three mutually perpendicular directions, which gives the resulting scaled-down ball, i.e., the same phenomenon as the contracted central ball-node in the muon. So, general relativity is applicable to describe (explain) not only the shell nodes flattening (including the direction of this flattening correctly) but also the central node's 3D-contraction. Further justification of the third variant through general relativity framework is deemed for future research; let us return to directly the negative energy calculation.

The negative (expended) energy, E_{neg} (on compression of a node) is equal to the difference between (energy of) the final and the initial momentum (e.g., for (26), it is $4 - 1 = 3$, and in the masses of the electron, $E_{neg} = 3 \times 4 = 12$). Thus, the formula for computing the total negative energy (i.e., for the whole construction) is as follows:

$$E_{neg} = -\,[4n\,(1/d/d_1/d_2 - 1) + 4_{n1}(1/d_3/d_4/d_5 - 1)], \qquad (30)$$

where d, d_1, and d_2 are the diameters of the central node, along the x, y, and z coordinate axes, respectively; analogously, d_3, d_4, and d_5 are the diameters of the shell node, also along the x, y, and z coordinate axes, respectively (herewith, if flattening of a node is accounted, we choose the node whose center is on the x-axis e.g., the non-dashed node in figure 2, so flattening can be described by multiplying f only on (initial) d_3; negative energy for every shell node is obviously the same, so our choice of that node is eligible); 4 is the coefficient of conversion of energy into units of electron masses; n and n_1 are the number of nodes of a given type ($n = 1$, since it means the central node; $n_1 = 12$, i.e., 12 nodes of the shell); "−1" corresponds to subtracting of the initial inherent momentum or if (27) is considered instead of (1), "−1" is interpreted as subtracting of the initial mass; 1 in the numerator is the constant from (1).

It is noteworthy that the momentum can take values of < 1 if the diameter of a node is allowed to be > 1, but the momentum is 0 only if the diameter of the node reaches ∞ or if the second variant noted above is considered.

When the shell nodes are flattening, i.e., $f < 1$, if they stay in their place (i.e., their centers), they (nodes) cease to be in contact (unlike the original balls). Bringing them into contact again can be done by making it possible for the nodes to fall toward the center of the construction and thus approach each other until contact; at the same time, the scale of the rectangle in figure 4, in the corners of which the centers of the shell nodes are located, is reduced. The coefficient, k, in percent divided by 100%, by which the scale of this rectangle is multiplied (and accordingly multiplied the distance r (that is initial distance) from the center of the central node to the center of (any) node of the shell), was obtained (raw: in percent) using the vector graphic editor Inkscape (version 0.92.3), up to the third decimal place (the maximum that is allowed by this program), using also the maximum magnification available in the editor (25 600%) up to the visually determined contact of (borders of) ellipses (representing the projections of the flattened nodes of the shell), with the minimum possible thickness of the ellipse border = 0.001 mm (the dimensions of the figures were also set in mm,

with the maximum available precision up to three decimal places, i.e., (here) with 6 significant digits).

The obtained coefficients k for the values of f considered in this paper are as follows: see table 1. The geometric coefficient k is considered not only in the calculation of positive energy i.e., when computing components l_1^2–l_4^2, see., (6), but also in calculating negative energy since the diameter ($d = d_2 = d_3$) of the (shrinking) central ball-node is linked to the shell node center's final position; this diameter is as follows:

$$d = 2(rk - 0.5f), \qquad (31)$$

where rk is the distance from the center of the central node to the center of the flattened node of a shell after the latter comes into contact with other flattened nodes (i.e., after they fell toward the center); f is the deformation parameter of the shell node (of compression along the direction to the center of the structure).

f	k
0.98	0.99451
0.97	0.99178
0.96	0.98909

Table 1: Dependence of the Geometric Coefficient k on the Flattening Parameter of the Shell Nodes, f

To obtain E_{neg} when the scale of the whole construction decreases (s <1), each diameter in (30) should be multiplied by s. A (mathematical) stencil summarizing the formulas for all 4 types of distances squared and for the accompanying sums of energies of bonds (E_1, E_2, E_3, and E_4) was used to start calculations at each iteration. You can find the stencil in (or as) Supplement 1. The stencil also contains fields to be filled with the sum of E_1–E_4: $E_{positive}$ (of the construction) and E_{total} (the sum of positive and negative energy), i.e., the mass of a muon whose value varies from iteration to iteration; these masses can then be analysed in a statistical program, while obtained distances squared (saved, e.g., by putting in their values in place of calculated appropriate formulas, as in Supplement 3, which contains 100 filled stencils) are additionally useful for computing cases with s <1: in this type of calculation, a square root is first applied to extract distances l_1–l_4, each of which (as mentioned earlier) should be multiplied by s and then returned to squared form, needed for further computations.

Supplement 2 contains the list of random numbers (i.e., the sequence of π, broken on separate numbers) that were utilized for each of the 100 iterations. The "replace all" option in the Notepad application (Windows, Microsoft Corp.) was used to manually, repeatedly, substitute intermediate results of calculations into the stencil. The raw results of calculations (of 100 iterations; see Supplement 3 for the (raw) data) were further prepared to form input for a statistical program and processed in the program Statistica (Stat Soft, Ink.; version 10) for the determination of the mean mass and the standard error of the mean (SEM). As 14% of scientific articles do not provide information about what measure of variability they use, i.e., whether it is standard deviation (SD), SEM, or other, the question of justifying the use of SEM (instead of, e.g., SD) may be considered non-important [123]. Let us, however, briefly state why SEM is used in this article: SEM is a measure of how far the population mean (i.e., here the final theoretical mass of a particle with infinite number of iterations) probably can be from our sample mean (i.e., of 100 iterations); i.e., SEM is able to show how precise our computation of theoretical muon mass is. (Precision is not to be confused with accuracy, which can be seen from comparing the mean with the experimental mass).

Another reason to use SEM is that, in contrast to SD, it tends to decrease with increase of sample size, i.e., it gains more zeros before significant digit(s); since the number of decimal places in error dictates how many of them should be expressed in the mean (for consistency and according to convention), and accounting for rounding to two significant digits (see details below), SEM allows to report more accurate value of the mean, if the mean actually converges (with growth of sample size) to the observed value (mass). (The sample grown to 100 already allows SEM to give one more digit after the point when reporting value of the mean in conjunction with SEM.) Other considerations why SD is irrelevant to provide (compared to SEM): values of muon's mass obtained in each iteration, the variability of which is reflected by SD, clearly (see the value of SEM in the 3rd section, and account that SD always ≥ SEM) do not correspond to masses that can be observed in experimental settings since muon is known to be an extremely narrow particle (in contrast to, e.g., resonances, Higgs boson); particle width, Γ, of muon, computed from its lifetime, τ, by well-known relation $\Gamma = \hbar/\tau$, where $\hbar$ is the reduced Planck constant in eV × s (with value from the literature), is ≈ 3×10^{-10} eV, which, divided by electron mass in eV, gives muon's width as just ≈ 0.6×10^{-15} electron masses [2,124]. (Physical interpretation of muon masses obtained in separate iterations is generally beyond our scope).

The SEM is reported rounded to two significant digits, which is consistent with the way error is given in the experimental mass; the mean is rounded to the number of decimal places that match that in the error [2]. For a degree of rounding, we chose between rules used by two sources dealing with the representation of particle masses: The Particle Data Group, PDG (2022), which rounds error with the highest order digits 355–949 to one significant digit, and the Committee on Data of the International Science Council, CODATA (2022), which rounds to two, i.e., with less information loss but producing less convenient (bulkier) value [2,124]. In summary, the first source offers only a more convenient view of a result, compared to the consistency with error in the observed mass, and less information loss offered by the second, so we chose the second. Exception: in tables 2-4, rounding of the mean was performed in accordance with the error rounded to 4 significant digits, i.e., to the 3rd decimal place, which, in table 2, is the very minimum required to capture the position of the mass-energy maximum when varying s (and in the other tables is for consistency).

3. Results

Tables 2, 3, and 4 represent the mass-energy calculations with three different values of the compression of the outer nodes along the direction to the center of the construction (f = 0.98,

0.97, and 0.96), each under the set of values of the scaling down (compression) parameter of the whole structure, in steps 0.01 (s <1), in comparison with the uncompressed construction (s = 1). (These steps are of 1% of the uncompressed structure; the steps in f are also of 1% but of the (uncompressed, more preciselyun-flattened) node (f = 1); in other respects, the choice of the value of the steps is arbitrary).

As can be seen from the tables, it is possible to determine the position of the maximum of the mean of the total energymass (corresponds to f = 0.97, s = 0.94). (More precisely, the identified maximum is a lower bound on the real maximum; refining the position and magnitude of the latter requires calculations with (progressively) smaller steps in f and s). The observed maximum (its lower limit) replicates the muon mass to the first decimal place: 206.7 (±2.5) electron masses compared to the experimental mass of 206.7682827(46), and is 100.0% (±1.2%) of the latter. Let us, additionally, estimate the value of the real maximum (and thus the (non)importance of the limitation in the steps' value): in the simplest way, it can be done using the numbers from table 2,which (represented with a smaller number of significant digits) are 206.70, again 206.70, and 206.60; the peak (extrapolated), obviously, lies (in the middle) between the two 206.70 values: 206.75 masses of electron; on the graph, this peak will be sharp (imagine, e.g., the right angle), which is not realistic for quadratic and cubic functions, so the real peak should be (in the simplest treatment) <206.75, yet >206.70; in other tables, the mass values are not symmetric (in contrast to 206.70's), so these cases are omitted from our estimation, for simplicity (but we account that all values in these tables are <206.75); in summary, the real maximum's estimate (206.70 < x <206.75, i.e., = 206.7) coincides with the maximum (of the mean) given above (i.e., the maximum from comparing the masses in all the three tables, which (maximum) at the same time was the lower limit of the real maximum), thus justifying the reported central value of muon's theoretical mass (however, not concisely, which is one of the limitations of our work). (Note: the estimate should not be confused with the real maximum with ∞ iterations, the estimation of closeness to which, through closeness to 206.7, is depicted by SEM.)

s	m
1	204.898
—	—
0.94	206.700
0.93	206.703
0.92	206.597

Table 2: The mass (mean), *m*, of the structure (in electron masses) with the deformation parameter (value of flattening of the shell nodes) *f* = 0.98 and varying the scale factor *s*

Even though we were able to obtain a coincidence between the theoretical and experimental masses up to the first decimal place, considering the high degree of uncertainty, we do not yet claim that the muon mass is explained theoretically to this decimal place. The calculations have shown that our model provides at least a good approximation to the observed muon mass after accounting for uncertainties. The justification for using the term *good* is that all possible masses (in range ±1 SEM) deviate from the experimental mass (EM)if accounting for one significant digitno more than 1%: EM (±1.2%), which approximately (due to EM does not precisely coincide with the theoretical mean) can be seen from the aforementioned 100.0% (±1.2%); in both representations, values are in percent of EM (the latter has value 100% (exact number, because EM is the reference), while theoretical mass 100.0% has implied uncertainty of half of the least significant digit, i.e., (uncertainty) 0.05%, not to be confused with SEM); note: the coincidence of the value of error around EM (derived (error) from SEM and the difference of EM and the mean) with the value of SEM is due to the closeness of EM and the theoreticalmass; if it were not such closeness, the error around EM would be asymmetric or EM would lie outside its whole range [39]. And the phrase "at least" is due to the possibility of making more than 100 iterations (in future work using the model) and thus decreasing error (due to SEM (as was said) shrinks with increasing statistics), which may shift the mean (i.e., theoretical mass), including toward (to be even closer to) the observable mass.The measured muon mass with its error is within 1 standard error of the calculated (and partially estimated) mass.

s	m
1	205.058
—	—
0.95	206.664
0.94	206.716
0.93	206.692

Table 3: The mass (mean), *m*, of the construction (in electron masses) is calculated using the value of flatteningof the shell nodes *f*= 0.97 and the variable scale factor *s*

s	m
1	205.200
—	—
0.95	206.681
0.94	206.714
0.93	206.660

Table 4: Mass (mean), *m*, of the construction (in electron masses) with deformation (value of flattening of the shell nodes) *f* = 0.96, and varying *s* (the scaling factor)

4. Discussion

In the Mohapatra model, Terazawa-Chikashige-Akama formulas, Georgi and Nanopoulos equation, Barbieri-Nanopoulos model, Terazawa model, Koide formulaand its modification and in other models,the mass of the muon can be calculated from the known experimental masses of other elementary particles (or such with the addition of bounds on (neutrino) mass(es)(a muon's mass can be computed with the "≈" sign)differences of squares of mass eigenstates (of neutrino)not absolute massesare also available; orfrom the upper bound on (neutrino) mass; or from the masses in higher (not reached yet) energiesin the Georgi and Jarlskog model, Barbieri-Nanopoulos modeland note that models(results) in high (not reached) energies can be extrapolated (renormalized) to laborato-

ry energies [6,7,13,14,16,17, 19-21,25-28,36,38,43,44,47-52,54-57,59,61,62,73-77,83,86,88,89]. In the Nambu formula, and other models, the calculation of the muon mass (in the form of Yukawa constant for interaction with the Higgs field for muon) also includes a parameter measured experimentally: the fine structure constant (in the Horning formula, Mirman formula, Ivanter's model, Barr and Zee models, Nambu-Barut equation, model of Barbieri and Nanopoulos, Barricelli's model, and other models, in addition to other theoretically unexplained constants of nature including particles' masses) [4,5,7,9,10,15,18,19,24,29,33,35,37,48,63,64,66,68-72,78,79,84,91]. A number of modelsutilize other experimentally measured constants of nature (or combination of such (or bounds on them) with the masses: the Heisenberg formula, Ivanter model, Kumar–Muthanna–Sinha formula, one of the Koide's equations, or use (also deemed as experimental) constants, calculatedor likely calculatedfrom particles' massesincluding that of muon, so theoretical mass of muon in allthree cited sources (describing 4 models) is computed (see below) not independently of its experimental mass) [6,7,10,11,14,21,23,31,34,40,42,45-47,49,56,65,67,77,81,84,90]. Many of the models are empirical(somesemi-empiricalor at least contain empirical partsnot counting the use of the constants, the (upper) bound on neutrino mass, etc)[5,14,20,21,26,31,37,43,45,48,50,52,60,61,64,75,86,125]. In contrast to all of these models, our model does not use any experimental quantities in the calculation of mass, i.e., if it can be said, mass is calculated from the first principles: geometrical relations and potentials of the simplest form describing the forces of attraction and repulsion.

As a result, the precision of the calculation of mass of the elementary particle using our model is limited not by experimental data but only by the number of iterations performed. Thus, with an increasing number of such, one can expect not only the possibility to reproduce completely the known experimental mass but also to give experimentally verifiable predictions (e.g., about further decimal places in the muon massnot reached by the available value from experiments).

In Koide's report, and other sources, the experimental mass of the muon (together with the mass of the electron and other particlesproton and neutron, quarks in one case and W boson in another, and (constraints on) neutrino (masses)) is used to calculate the mass (or its lower bound) of the heavier analog of the electron, the tauon, rather than the opposite [22,26,28,59,76]. Similarly, in the Goldman–Vinciarelli, Georgi and Nanopoulos, Barbieri–Nanopoulos, Terazawa, Koide's and in many other aforementioned worksonly presented formulas (models) in the framework of which the muon mass can be deduced (based on observed other particles' masses or masses that may be observed in not yet reached energies or based on other fundamental natural constants, including hypothetical ones), but the actual calculation of such mass was not carried out [12,14,16,19,20,23,25,27,38,41,43,44,47-51,53-57,61,62,69,70,77,80-83,89]. The muon mass in the literature, up to now, has been theoretically calculated as matching with the experimental value to at most 1 decimal before (not after) the decimal point (if not taking into account the exceptions criticized below), and the obtained values (in electron masses) are 218.76 (Darling model), 206 (Nambu formula, in original (1952) letter; the same is the modern value in similar model [78]) [5], 200 (Heisenberg formula) [6,7], ~ 202 (Horning solution) [4], 207.0595 (Mirman formula) [9], ≈ 208.5 (Ivanter (topological) model) [10], 180 (Kumar–Muthanna–Sinha model) [11], 206.5539987 (13) Nambu-Barut formula [84], 208 (in two different cases)Barricelli model [24], 206.69 [71], 206.56 [126] or 206.554 [126] or 207 (twice) [91], 206.55 [66], 207 [64], 207.05385 [29], 206.356610 [60] or 206.34 [58], 208 (twice) or 205 or 206 [39], 205.56 [35],208(10) [14], 205.5 [87] or 204.6564531 [73], 205 [34], 204 [52], ≈ 203.9 [21], 210 (three significant figures) [6], 210 [63], ≈ 210 [49], 202 [33], 198.8 [30], 220 [18], 220.08 [42], 220.2 [72], 185.2 [74]. In [74], the value (of 0.169) used in the calculation of mass is the value rounded non-conventionally; if, even not applying convention but not rounding the original value (0.16969...) since it is an intermediate result (and also applying the proper count of significant digits to the final result: hereone digit, due to "0.16969..." is an average from numbers having one–two of such), the mass would be 200 instead of 185.2. We have checked the value 205, according to the formula [34].

Other cited masses were not checked. In-depth analysis of existing models is generally outside the topic of the present work. Note: Many of the masses were converted from MeV or MeV/c^2 (by dividing by the experimental mass of an electron in MeV or MeV/c^2); the number of significant figures in these cases is the same as it was in one of the values with the fewest significant figures; (the MeV or MeV/c^2 mass of an electron was taken from the same cited source, and only if the latter mass was not listed or the authors of the source are not the authors of the model under consideration, the value was used from the review of the PDG) [124]. MeV and MeV/c^2 notations are used in the literature interchangeably, for mass of muon, and MeV notation also for equivalent (to muon's mass) energy [2,34,125]. (Whether MeV is mass or energy? Since (aforementioned) massenergy equivalence, all uses can be viewed valid.) Note also that in natural units, MeV equals MeV/c^2. Note: results, one arithmetic operation away from the mass, not counting conversion to electron masses, were considered calculated and, finalized, included in the list. (Not listed are masses calculated at the M_Z scale, etc.; these are treated as not calculated) [41,82]. Note: all masses, both experimental and theoretical, and their errors, cited from the literature, are expressed in the paper without rounding. (Note: all cited masses are in units of experimental electron mass: in many cases this was the only variant, and in others is for consistency (better comparability); in the abstract case, where both theoretical electron and muon masses (in some model) are precisely wrong, the representation of the muon mass in units of theoretical electron masses can be more correct if both masses are affected by systematic error (their relation can stay accurate); so, at least from this, it is not ungrounded to use theoretical electron masses also, but such a task is left for the future, e.g., for a(comprehensive) review article).

Although in the model [84] a result of 206.768282(12) is reported, it is calculated with a formula that already contains the ratio of experimental muon to electron masses, so the result can be regarded as adjusted; the same may be true for model [37], in which the method of derivation of the equation is not

disclosed and the calculated mass is very similar: 206.7682822; in [31], the result is 206.7693, also based on a formula with empirical value as an input (as a constant, a mass of 313.85773 MeV is given); also, other empirical formulas can be criticized from the same position, albeit they contain round numbers (or their relations) close to mass relations and not mass relations directly (one Koide formula) [26,84]. Also, all other empirical models can be criticized as adjusted (to an experiment) as they are (likely) developed not from theoretical reasoning but from the coincidence of calculation with experiment, which is the meaning of *empirical*; in one of such, the calculated mass is 206.7703, and in yet another one, it is 206.78852 [45,46,127].

In [32], the computed value of 206.7607796 is also very close to experimental, however, it has been chosen from a (dense) spectrum of values (which imply "more than a thousand light particles between the electron and muon"). Muon theoretical mass is 206.761078 in [40] and is explained as a combination of 6 = 3+3 fundamental masses of two types, but the numbers in the mass formula are not explained and thus can be free parameters. The same is true for [68], where the computed mass is 206.7. Also unexplained are the values of indexes in the formula that give muon mass as 206.75 in [67]. In the same way one may see the masses 206.766457 or 206.7671818, obtained in [79], and ≈ 206.764 in [86]. The result 206.84(38) is referred to a paper in preparation in [85] (notes: "8" (at first decimal place) also coincides with value in the experimental mass but if the latter (mass) given rounded to that (one) decimal place; 206.84(38) is further from (not rounded) observed mass than any of (actual and numerically possible) masses with "7" in the first decimal placeif not accounting for the uncertainties).

Within the 1σ range of the experimental mass are theoretical masses 206.7682786 in [65] and 206.7682830 in [36]; however, in the first source, at least some parameters in the mass formula are free, i.e., not justified by theory (if not counting that their choice is restricted to integral numbers and that some logic in their values was found postfactum), and in the second model, the bonding energies of sub-particles that constitute muon, and therefore the energy that they contribute to the particle's mass, are obtained from experimental masses of elementary particles, including muon, so the calculated mass is clearly adjusted. Note that the contribution of bonding energies to mass here is positive, as in our model (but note that our model is not built upon any existing models; however, (2023) has priority in introducing the positive contribution—of binding energies of constituents or sub-particles of muon) [36].

In contrast to these models, our model contains neither (as was previously mentioned) experimentally determined nor adjustable parameters, unless one considers the choice of cubic dependence instead of quadratic (the latter is the simplest among non-linear) for modelling the delocalization of a point in the node; choice is not justified by theory if not counting one insight on the physical origin of this dependence (see below). All possible dependencies of density distribution are contained between 0^{th}-power law (i.e., when all density is on the surface of a ball-node) and power $+\infty$ (i.e., when all density is concentrated in the center); the third extreme case is uniform densitysomewhere in between these (0 and $+\infty$) powers. It is assumed that all possible power dependencies of density distribution (excluding the 3^{rd} power) give at least an approximation to the mass of muon (while the 3^{rd} power gives an exact mass). If this assumption is correct (which requires calculations for proof), the theory is valid not depending on the power value, so the latter cannot be a free parameter of the theory even when "if" (mentioned above and to be discussed later) is not considered. The laws that govern attractive and repulsive forces between the nodes in our model are justified as being the simplest and having physical analogs (i.e., the force of gravity (and electromagnetism) for attraction and the Heisenberg uncertainty principle for repulsionalso shown described by special relativity).

It is worth mentioning that in conditions where the nodes are connected by nondirectional and thus spherically symmetric and non-saturable forces, i.e., similar to those presented in our model, which is true for metals and noble gases, the formation of densest packings of spheres (or balls, hereatoms) is advantageous, including, in the case of a small number of atoms (up to several hundreds to thousands, including the case of n =13 atoms), as shown in calculations and experiments, clusters with icosahedral symmetry, i.e., similar to the construction in our model. These further grounds (from analogy) the icosahedral arrangement of nodes as the lowest energy state (among other imaginable arrangements) and also adds to the explanation of n = 13 for the nodes (not 12 or 14, etc.) in the structure of muon; it also helps to explain the jump in the charged lepton spectrum (including in mass) from electron to muon, i.e., the non-existence of leptons intermediate between electron and muon [128-138].

Icosahedral, with n = 13 atoms, clusters are shown to be able to unite or interpenetrate to form poly-icosahedral structures [135]. (Interpenetration may be expected to occur through atom-by-atom growth, i.e., not as a result of the interaction of already-formed clusters (at least they seem not to move with high enough speed to interact non-elastically); two clusters may have one or more common atoms (it is geometrically possible)in some analogy with common electrons in molecules). Anyway, from observation of the poly-icosahedral structures, n = 13 icosahedral clusters of atoms can be viewed not only as repeating ball shape on a larger scale but also as behaving as balls: they do not merge with one another (at least completely), which is in line with our concept of the existence of 2^{nd}-order balls.It is noteworthy that our model calculations show that the case when both the center node and the shell nodes deform, albeit to different degrees, is energetically advantageous. The negative energy (i.e., the energy due to deformation) in electron masses per node is 0.96 for a shell node and 2.26 for the central particle, which is equivalent to a higher momentum of the central particle compared to the shell particle and allows to draw some analogy with a number of natural objects: neutron stars, white dwarfs, ordinary stars, and planets, in which the pressure and momenta of particles also grow towards the center. Thus, the object considered in the model has physical analogs in this respect.

The idea of a finite-sized ball, used in the model as a node of the construction, if compared with an object close in scale: the s-orbital of an electron, can be just an approximation to reality

(simplification), because the s-orbital has no boundary (electron density is distributed throughout the universe), although the overwhelming part of it is contained within a limited volume (for example, 95% of possible positions of an electron are inside a sphere of radius 1.7 angstroms) [139,140]. By analogy, the finite-sized ball considered in our model may also contain the vast majority of the point's positions, and thus its use in the model is, in this case, justified (in addition to the arguments in the 1st section).The fact that we consider, as realized in the ball-nodes, a non-uniform distribution obeying specifically the law of inverse cubes, (somewhere) intermediate between two extreme cases: uniform distribution (along the axes) and singularity (point), requires an explanation (mechanism). Interestingly, the stress created by a point defect in a crystalline lattice decays as $1/r^3$ with the distance r to the point defect [141]. This may be relevant in the search for a cubic dependence mechanism, the discussion of which is beyond the present scope.

Until the mechanism is found, the proof of the correctness (physical significance) of the dependence chosen in our model should not be only the reproduction of the muon mass but also the simultaneous (i.e., with the same law of density distribution in the nodes) obtaining of the mass of an even heavier electron, the tau-lepton; tauon mass is now calculable (see below). The question about the (quantitative and qualitative) relationship of the cubic dependence of the density distribution in the construction's node with the laws of the distribution of density of constituents in known natural objects with spherical symmetry, especially in atomic s-orbital and astrophysical objects, has not been studied: how much the density distribution law in these things resembles the cubic dependence (i.e., how common and natural this dependence is).

An example of a structure where the massenergy of the elements is small relative to the energy-mass of the forming system is baryons (objects formed by strong interaction), described simplistically as a bound system of three elements (three quarks) [1,124,142]. For instance, in the case of a proton, the masses of three quarks contribute only 1% of its mass [1,124,142], and thus are almost negligible. The massless nature of the bound elements (nodes) considered in the first variant in our modeli.e., in (1)is a limit case and may be an acceptable simplification. Also, nodes, as new objects whose nature remains to be understood, may represent states that do not interact with the Higgs field and thus do not receive mass in the first place. (Priority in introducing massless sub-particles in muon and charged leptons is of [65] (2012); however, note that in our model, the concept was introduced independently; note also that the muon mass models (our and [65]) are not similar).

As for the systems formed due to three fundamental interactions other than the strong (as well as due to non-fundamental forces, for example, the strong nuclear interaction), the binding energy makes a relatively small, relative to the masses of the bound elements, and negative contribution to the mass of the system (the so-called *mass defect*). In our model (and [36]), the contribution of bonds is positive, the reasons for which are not speculated in this work.To justify the lack of contribution of the possible mass of nodes to the mass of the construction, one can also speculate that instead of moving the considered structure in space, only the bonds and deformation of the nodes move (or the packet of useful energy released during the formation of the structure), so the nodes do not move, i.e., as in a wave: that the muon is a (nonlinear, particle-like) wavesoliton, in accordance with the way elementary particles are considered in solitonic models; the specification of this idea may be a topic for future research [143-145].

As was partially treated before, beside the direct verification of the model, an indirect verification is possible: by calculating, on the basis of the same idea and assumptions used in the model (i.e., using the same (general) approach or method), the mass of the 3rd-generation particlethe tau lepton, represented as a similar structure, but with two layers of nodes around the central one (in total, 55 nodes and 1485 bonds between them, versus 13 nodes in the muon and 78 bonds between them). Note: objectively, the general approach (mentioned above) is the approach for muon, but after deleting specifics of muon: number of nodes (i.e., 13): models for other fundamental particles are produced (not in details but overall) by considering other number of nodes; these numbers are not arbitrary, as seen for the tauon and as you can find for u- and d-quarks (and other particles)below. The general approach, initially, is the general theory (for many or all elementary particles); evaluation of its generality also according to experiment (i.e., check of correctness (generality) in practice) is below.

In continuation of the question of indirect verification of the mass model for muon, and as a (solution of a) problem that has a value on its own, and to start evaluating the (practical) generality of our approach, we report here the results of calculations of tauon mass for the doubly simplified case, namely, where attraction is computed only between the centers of nodes (i.e., no delocalization of a point is calculated), and in the computation of negative energy (or repulsion), the 1D-case is considered, namely, the distances between the nodes' centers instead of (shrinking of) the node's dimensions (i.e., the formula $\Sigma\{[(1/l_a)-1]na\}$ is applied, where la is the distance (of different types, a) between the centers of nodes (only l_a's<1 are eligible for the formula); n_a is number of such distances in the construction): in such a case, spontaneous collapse of the 55-ball structure gives (a lower bound on) the maximum of the energy-mass as 3408.17 electron masses, which should be compared with the experimental value of 3477.23(23) [2]; i.e., the theoretical mass of tau is (at least) 98% of the observed. The second simplification (above, i.e., in the negative energy calculation) can be viewed also as another method to calculate E_{neg}since 1D is applied not to the node's dimensions. If viewed so, the question of incomparability between the models arises. It poses a task for the future to calculate tauon's mass with treating E_{neg}as in muon's case. (Note: the mass in percent here is rounded to whole numbers, for convenience; if not rounded, it is 98.0140%). So, it is shown (at least partially) that our general approach is applicable to other particles than muon: at least it (possibly modified if considering the probable incomparability nuance) gives a close approximation to the tau-lepton mass (from the lower bound), which indirectly verifies the muon mass model. (Furthermore, the lower bound here, of the real maximum, as was(indirectly) mentioned before, is

attained when all the distances in the tauon shrink to the half of initial ones, so all the distances that start from = 2 (78 distances are of this type) are now = 1; accounting that the rate of energy release approaches maximum when the points approach distance = 1, and that all probed energy-masses for $s <$ and >0.5 were lower than 3408.17, it is assumed (grounded) that 3408.17 is the real maximum; the latter not to be confused with global and real-maximum-in-general (i.e., outside the simplified case); globality of the present maximum was assessed partially).

Further details of the model for tauon are omitted in this paper (i.e., the model is reviewed only partially, which complies with the title, which emphasizes the mass, not the model, in the tauon's case). We also (for similar reasons) do not give details of derivation of 3408.17 as mass-energy maximum (i.e., like with tables 2–4); this do not prevent the model and results from being verifiable and falsifiable.Interestingly, the diameter of the whole structure of tauon, D, compressed to the lowest energy state, is $0.5 \times 5 = 2.5$ (where 0.5 is the diameter of equal-sized balls (ball-shape is one of the possible interpretation of the distances between nodes' centers) and 5 is the number of ball-nodes in the 1D slice of the structure in the widest part, which equals the diameter of a circumscribed sphere that touches the surfaces of the nodes), while for muon, $D \approx s[f + 2(rk - 0.5f) + f]$ (for $f = 0.97$, $s = 0.94$, and corresponding k from table 1; r from Supplement 1) = 2.7. So, the more massive, with more nodes, structure has dimensions smaller than the structure less massive, with fewer nodes. White dwarfs and neutron stars also shrink with more mass and matter (i.e., a more massive white dwarf has a lower volume than a less massive one; so [107] (but still discussion able [146]) for neutron stars); from this analogy, our models get additional grounding: analogy with known natural objects (white dwarfs and neutron stars) is more than in the rise of momenta with depth.

When adding an electron, $D = 1$, to muon–tauon sequence, one can see that initially, dimensions grow with mass and matter (to $D \approx 2.7$ in muon), in analogy with, e.g., in planets (more and more massive), and only then start to shrink, so, repeating the natural law, seen in the sequence (of growing mass of) planets–post stellar objects (white dwarfs, neutron stars). So, in our models (of electron, muon, and tauon), this law is repeated and adds to the justification of our theoretical constructions. (One can see that the volume–mass dependence is reproduced not only in muon–tauon sector, but for the whole sequence.) Note: post stellar objects also include black holes—for which, sizes, with current physics, are zero, i.e., singularity (in a limit—non-rotating, non-collapsing case); these objects lie along the upper part of the volume–mass dependence; the corresponding (i.e., the upper) part for charged leptons' sequence is linked to the mystery of the non-existence (non-observational status [124]) of 4^{th}-generation charged leptons (and that of higher generations). Is this somehow connected to a black hole, or does it have another mechanism? The question is out of the scope of the present work, as it is not directly related to the topic (see the title)and can be addressed, e.g., to an interested reader. We, however, announce the hypothesis of the mechanism for the 4^{th}- and higher generations' charged leptons' non-existence; also, there are mechanisms proposed in the already cited literature in this paper [75,76,92].

To better comply with the plural "applicable to other particles" (said above, about our general approach, in the sense of: in practice), we also report here the masses of the elementary particles from another group than charged leptons (electron, muon, tau): of a quarks. First, we consider the simplest case, i.e., the lightest quark: u-quark. The simplest possible construction after an electron (one node) is two interacting, contacting nodes (in comparison with charged leptons, such a construct is non-spherical and not close to a sphere by symmetry). Adding to the first simplification described for the tauon mass calculation, the secondbeing non-compressibility, we obtain a trivial result, already shown in figure 1: 4 electron masses (exact number). The observed u-quark mass is 4.23 (+0.96/−0.51) masses of electron [124]. So, the mass of the up quark, in a doubly-simplified case' calculation, is well within 1 SD of experimental. This further, indirectly, justifies the physical significance of the application of the general method to muon's case (i.e., the model of muon mass).

The simplified mass of the second lightest quark, d-quark, can also already be seen from figure 1, and equals 9 masses of electron i.e., the energy-mass of three interconnected nodes, which is the next simplest number of nodes after being used to describe u-quark (so, one can see that the number of nodes is not arbitrary). A model for the down quark, according to figure 1, contains three simplifications, two of which are the same as for the up quark, and the third is due to the arrangement of nodes being considered only as 1D, while for the down quark also possible are 2D arrangements (i.e., triangles). Observable d-quark mass is 9.14 (+0.94/−0.33) [124]. So, the theoretical mass of down quark is also well within the 1σ experimental range.

The experimental masses of electron, u- and d-quarks resemble a sequence 1,4,9 [30]; now we have a theoretical explanation of this phenomenon, in addition to other theories that can be found in the literature. Theoretical masses of u- and d-quarks as 4 and 9 electron masses are already given in [147] (2020), with an alternative (to our approach) explanation of this matter.Existence of heavier quarks can be understood in analogy with $u^{2/3}$ and $d^{1/3}$ quarks: charm, $c^{2/3}$, and bottom, $b^{1/3}$, quarks are constructed of also two and three but 2^{nd}-order balls, respectively; top, $t^{2/3}$ quark—of two 3^{rd}-order balls, which non-trivially predicts the existence of an even heavier quark (made of three 3^{rd}-order balls), with the 1/3 charge (one "if" can prevent the existence of this, 4^{th}generation, quark; whether this "if" works is checkable by calculation). Omitted to this point was the strange, $s^{1/3}$ quark: its hypothetical mechanism of existence (not to be discussed here) is slightly not in line with the simple scheme for other quarks (but is (of course) still within our general approach); this theoretical "not in line" explains why this quark's observable charge and mass disrupt the simplicity of the experimental sequence of quarks if it had been without s-quark: one can expect that after $d^{1/3}$, a quark with charge 2/3 should follow, but $s^{1/3}$ is intervened; also, one should expect masses of 2^{nd}generation quarks to be close to each other (as is known for the 1^{st}-generation quarks, with experimental mass ratio 2.11 (+0.25/−0.33) [124]), but

the s-quark is much lighter than the c-quark (mass ratio from experiments: 11.76 (+0.05/−0.10) [124]); nonetheless, both of these quarks are termed 2nd-generation quarksand this can be reasonable accounting for the values of elements in the Cabibbo–Kobayashi–Maskawa (CKM) matrix [124]. One can see that in the 2nd generation, quark with charge 1/3 (s-quark) turns out to be lighter than that with charge 2/3 (c-quark), while in the 1st generation it is the opposite ($u^{2/3}$ is lighter than $d^{1/3}$), so the (enigmatic) inversion is seen. Everything falls into place when one considers the mechanisms mentioned above, which show uniqueness of $s^{1/3}$ along with the closeness of $c^{2/3}$ to $b^{1/3}$ (analogous to $u^{2/3}$ to $d^{1/3}$)which can explain, at least qualitatively, (small) experimental b- to c-quark mass ratio of 4.58 (±0.01) [124]; the samefor $t^{2/3}$ quark: while its observed mass ratio to another 3rd-generation quark, $b^{1/3}$, is 41.3 (calculated from the central values [124])compare with 2.11 and 4.58, ratio to the predicted 4thgeneration quark should be relatively small: from linear extrapolation (continuation of the sequence: 2.11, 4.58, x) it is 7.05, which gives (with t-quark mass of 172.69 GeV [148]) the mass of the new (awaited) quark as 1.22 TeV; this mass should be compared with the lower bound (experimental) in searches of a possible 4th-generation quark, b', with charge 1/3: >1.57 TeV [124]; so, the simplest (linear) extrapolation excludes our predicted quark. However, there is a sign of non-unitarity of the CKM matrix (in the first raw) with 2.2 sigma significance [124], which, if it will rise to at least 5 sigma's (with future experiments), will certainly imply the existence of the b'-quark or other physics beyond the Standard Model [149]. (The statistical significance actually dropped from >4σ as it was in 2020) [149].

5. Conclusions

A new model is presented to explain the value of the muon mass (or muon–electron mass ratio)a model, which allows for the theoretical calculation of at least a good approximation to the mass of this elementary particle. A muon mass is computed as 206.7 (±2.5) electron masses versus the experimental value of 206.7682827(46), i.e., is 100.0% (±1.2%) of the measured mass. The mass is identified with the maximum of the released useful energy during the formation of a structure composed of 13 (deformed) ballnodes that (structure) possess the approximate symmetry of a sphere and can be viewed as a structure of the 2nd-order (also ball) in comparison with one node (the 1st-order structure, identified with an electron). This maximum (of mass-energy) in the paper was looked for by considering various possible values of flattening of the outer nodes and compression of the whole structure of already contacting ball-nodes. The maximum was obtained, i.e., the theoretical mass noted above. (The presence of possible additional (local or global) maxima was not tested in this work). The energy release in formation of the structure is limited by the establishing equilibrium of the modelled simplest forces of attraction and repulsion between the nodes.

The results are obtained based on 100 iterations of the algorithm, with substitution at each iteration of random numbers generated using the π number sequence. Going beyond 100 iterationsto 250, 500, 1000, etc., may be time-consuming (100 iterations took about a one-and-a-half month of calculations) but it will allow one to determine how many decimal places in the muon mass the presented model can reproduce (stable within 1 sigma) and to find out whether it is an approximation or an accurate description of the muon mass. Continuation of the calculations will also reduce standard error in the mass representation.The computations performed are limited by the accuracy of the coefficient k, determined in a graphical way (with the graphic editor Inkscape): there is a limitation of three decimal places in its displayed value and also in the process of obtaining this value by specifying the dimensions of ellipses (projections of flattened outer nodes). Instead of a graphical determination of k, the task of obtaining it in a mathematical (geometric) way, which may be more accurate, can be set.

Also, when working in the graphic editor and in calculations, the rounded value of the angle g was used (the accuracy of the rotation of geometric figures in the editor, in degrees, is limited to three decimal places). (The use of the rounded value also in the calculations ensures consistency). The calculations' precision can be increased by utilizing a more precise angle, which may be required for replicating the muon mass to the n^{th} decimal place. The model's calculations were largely performed manually, so their speed could have been greatly improved by the use of Keisan online calculator technology (Casio Computer Co., Ltd.), with functions to automatically substitute variables and solve long formulas, which is now discontinued, but it is possible that this technology could be repurchased or reproduced. (Our first algorithm was intended for this calculator; discontinuation of the latter in 2023 forced us to recreate an algorithm "from zero" for manual calculations (with use of only Windows calculator), described in this paper). The task of automating the calculation by means of a computer algorithm may also be posed.Thanks to the use of input data from the π sequence, known to 62.8 trillion decimal places, the computations of our model are well suited for collective (or distributed) calculations, where different authors consider different parts of this sequence [150].

The challenge of creating a three-dimensional representation of what can be viewed as muon's internal structure, presented in this paper only in the form of slices of individual pairs of nodes (the uncompressed structure's case) and a mathematical description, is also posed.The physical interpretations of the model, including the nature of the cubic dependence of the density distribution in the structure's node, have generally remained outside the scope of the present work.The task of calculation, with the general approach shown in the paper, of other particle masses, which will indirectly aid our muon case model, is set for the future, except for the masses of tauon, u- and d-quarks, reported in this work, obtained in the simplified cases. Particularly interesting is whether the masses of tau and quarks will (better) converge to the observed ones when moving from simplified models to concise computations [151].

Data Availability Statement

The data supporting the findings of this study are freely available and are placed in supplementary materials.

Acknowledgements

We acknowledge the 2013 publication [151] by R. S. Hundi and

S. Sen Gupta, which provided access to an even greater number of articles on the subject. We are also grateful for the reviewing work of Z. G. Berezhiani and R. Rattazzi (1993) in [54], from which we got a lot of cited sources.

References

1. Boya, L. J., & Rivera, C. (2011). On the masses of elementary particles. *Physics of Particles and Nuclei, 42,* 800-811.
2. Tiesinga E, Mohr P J, Newell D B and Taylor B N 2024 The 2022 CODATA Recommended Values of the Fundamental Physical Constants (Web Version 9.0) Database developed by Baker J, Douma M and Kotochigova S (available at: https://physics.nist.gov/ constants, National Institute of Standards and Technology, Gaithersburg, MD 20899).
3. Darling, B. T. (1950). The Irreducible Volume Character of Events. I. A Theory of the Elementary Particles and of Fundamental Length. *Physical Review, 80*(3), 460.
4. Horning, S. C. (1960). Mass of elementary particles. Nature, 186, 708.
5. Nambu, Y. (1952). An empirical mass spectrum of elementary particles. *Progress of theoretical physics, 7*(5-6), 595-596.
6. Varlamov, V. V. (2023). Group Theory and Mass Quantization. *arXiv preprint arXiv:2311.16175.*
7. Varlamov, V. V. (2023). ON MASS QUANTIZATION. *Metaphysics*, (1), 115-134.
8. Sakharov, A. D. (1968). Is there an elementary length? Physics in School, 2, 6-15.
9. Mirman, R. (1961). A postulated law for the masses of the elementary particles (No. NASA-CR-67390).
10. Ivanter, I. G. (1963). The topological structure of space and the mass spectrum of elementary particles. In *DokladyAkademiiNauk* (Vol. 148, No. 2, pp. 303-306). Russian Academy of Sciences.
11. Kumar, N., Muthanna, M., & Sinha, K. P. (1972, February). On mass quantisation of elementary particles. In *Proceedings of the Indian Academy of Sciences-Section A* (Vol. 75, pp. 57-67). Springer India.
12. Goldman, T., &Vinciarelli, P. (1974). Composite Higgs fields and finite symmetry breaking in gauge theories. *Physical Review D, 10*(10), 3431.
13. Mohapatra, R. N. (1974). Gauge model for chiral-symmetry breaking and muon-electron mass ratio. *Physical Review D, 9*(12), 3461.
14. Terazawa, H. (1992). How to solve the mass spectrum of quarks and leptons. *Modern Physics Letters A, 7*(21), 1879-1885.
15. Barr, S. M., & Zee, A. (1978). Calculating the electron mass in terms of measured quantities. *Physical Review D, 17*(7), 1854.
16. Georgi, H., &Nanopoulos, D. V. (1979). Ordinary predictions from grand principles: t-quark mass in O (10). *Nuclear Physics B, 155*(1), 52-74.
17. Georgi, H., &Jarlskog, C. (1979). A new lepton-quark mass relation in a unified theory. *Physics Letters B, 86*(3-4), 297-300.
18. Kyriakos, A. G. (2011). Nonlinear Theory of Elementary Particles Part XV: On Calculation of Elementary Particles' Masses. *Prespacetime Journal, 2*(12), 1933-1948.
19. Barbieri, R., &Nanopoulos, D. V. (1980). An exceptional model for grand unification. *Physics Letters B, 91*(3-4), 369-375.
20. Terazawa, H. (1980). Algebra of subquark charges. *Progress of Theoretical Physics, 64*(5), 1763-1771.
21. Sumino, Y. (2009). Family gauge symmetry as an origin of Koide's mass formula and charged lepton spectrum. *Journal of High Energy Physics, 2009*(05), 075.
22. Koide, Y. (1981). *Quark and lepton masses speculated from a subquark model* (No. SH-81-11).
23. Koide, Y. (1983). A fermion-boson composite model of quarks and leptons. *Physics Letters B, 120*(1-3), 161-165.
24. Barricelli, N. A. (1981). The masses of elementary particles calculated by a magnetic monopole model theoretic implication. *Preprint series. Mechanics and Applied Mathematics.*
25. Liang, Z., & Sun, Z. (2021). A modified version of the Koide formula from flavor nonets in a scalar potential model and in a Yukawaon model. *Nuclear Physics B, 972*, 115546.
26. Gao, G. H., & Li, N. (2016). Explorations of two empirical formulas for fermion masses. *The European Physical Journal C, 76,* 1-7.
27. Chen, M. C., King, S. F., Medina, O., & Valle, J. W. (2024). Quark-lepton mass relations from modular flavor symmetry. *Journal of High Energy Physics, 2024*(2), 1-28.
28. Wilson, R. A. (2022). Remarks on the group-theoretical foundations of particle physics. *International Journal of Geometric Methods in Modern Physics, 19*(11), 2250164.
29. Chiatti, L. (2009). A possible model for the mass spectrum of elementary particles. *arXiv preprint arXiv:0905.3794.*
30. Singh, T. P. (2022). Why do elementary particles have such strange mass ratios? The importance of quantum gravity at low energies. *Physics, 4*(3), 948-969.
31. Rosen, G. (2007). HEURISTIC DEVELOPMENT OF A DIRAC–GOLDHABER MODEL FOR LEPTON AND QUARK STRUCTURE. *Modern Physics Letters A, 22*(04), 283-288.
32. Sapogin, L. G., &Ryabov, Y. A. (2010). New theoretical results about the mass spectrum of elementary particles. *Applied Physics Research, 2*(1), 86-98.
33. Mashford, J. (2024). Erratum: "Computation of the masses of the elementary particles" [AIP Advances 14, 015007 (2024)]. *AIP Advances, 14*(3).
34. Olivi-Tran, N. (2020). Theoretical calculations of the masses of the elementary fermions. In *Accelerators and Colliders* (p. 73). intechopen.
35. Vasiliev, B. V. (2019). On the Nature of π and μ Mesons. *Journal of Modern Physics, 10*(1), 1-7.
36. Bondarev, V. G., &Migal, L. V. (2023). Computer modelling of material objects' structure: Part II. Elementary particles.
37. KUZNETSOV, A. (2017). Formula for the mass spectrum of charged fermions and bosons.
38. ElOkaby, A. A. (2007). A short review of the Higgs boson mass and E-infinity theory. *Chaos, Solitons & Fractals, 33*(1), 14-25.
39. Warmann, T. (2022). The generation of mass in a non-linear field theory. *ZeitschriftfürNaturforschung A, 77*(8), 723-798.

40. Meissner, R. (2014). Derivation of the Relativistic Laws of Force and Their Consequences. *Science Journal of Physics, 2013.*
41. Campos, M. D., Cárcamo Hernández, A. E., Kovalenko, S., Schmidt, I., & Schumacher, E. (2014). Fermion masses and mixings in an SU (5) grand unified model with an extra flavor symmetry. *Physical Review D, 90*(1), 016006.
42. Oldershaw, R. L. (2010). The subatomic particle mass spectrum. *arXiv preprint arXiv:1002.1078.*
43. Mangano, G., &Sannino, F. (1993). A Mass spectrum for leptons and quarks. *Modern Physics Letters A, 8*(16), 1519-1526.
44. Joaquim, F. R., &Penedo, J. T. (2014). Radiative charged-lepton mass generation in multi-Higgs doublet models. *Physical Review D, 90*(3), 033011.
45. Akiba, Y. (2019). Updated empirical formulae of the masses of elementary particles RIKEN Accelerator Progress Report 2018 vol 52 ed H Ueno et al (Wako, JP: RIKEN NishinaCenter for Accelerator-Based Science) p 98.
46. Akiba Y 2019 A model of the empirical mass formulae of elementary particles RIKEN Accelerator Progress Report 2018 vol 52 ed H Ueno et al (Wako, JP: RIKEN NishinaCenter for Accelerator-Based Science) p 99.
47. Raju, C. (2024). Tau and M-Neutrino and All Massive Leptons. *Ann Comp Phy Material Sci, 1*(2), 01-08.
48. Lipmanov, E. M. (2005). On lepton flavor mass-degeneracy-deviation hierarchies and QD-neutrino mass. *arXiv preprint hep-ph/0511266.*
49. Giani, S. (2012). Particle mass formulae. Phys. Essays, 25. 470.
50. Paasch, K. (2016). On the Calculation of Elementary Particle Masses. *Prespacetime Journal, 7*(12), 1597–1611.
51. Terazawa, H. (1990). Triplicity of hadrons, quarks and subquarks. *Modern Physics Letters A, 5*(13), 1031-1039.
52. Samsonenko, N. V., Haidar, R., &Alibin, M. A. (2022). DOES THE "GOLDEN RATIO" ARISE IN BARUT MODEL FOR THE PARTICLE MASS SPECTRUM?. Metaphysics, (1), 55-58.
53. Babu, K. S., & Mohapatra, R. N. (1990). Permutation symmetry and the origin of fermion mass hierarchy. *Physical review letters, 64*(23), 2747.
54. Berezhiani, Z. G., & Rattazzi, R. (1993). Inverse hierarchy approach to fermion masses. *Nuclear Physics B, 407*(2), 249-270.
55. Ibanez, L., & Ross, G. G. (1994). Fermion masses and mixing angles from gauge symmetries. *Physics Letters B, 332*(1-2), 100-110.
56. Binetruy, P., &Ramond, P. (1995). Yukawa textures and anomalies. *Physics Letters B, 350*(1), 49-57.
57. Dobrescu, B. A., & Fox, P. J. (2008). Quark and lepton masses from top loops. *Journal of High Energy Physics, 2008*(08), 100.
58. Arneth, B. (2021). Pythagorean numbers and the calculation of the masses of the elementary particles. *Physics Essays, 34*(3), 322-330.
59. Terazawa, H. (2011). Masses of fundamental particles. *arXiv preprint arXiv:1109.3705.*
60. Balogh V and Straub D 1998 Halbempirishemassenformel (HEMF): Quantitative darstellung der elementarteilchen-massen (B 01/1998). Institutfu¨rThermodynamik, Universit¨at der Bundeswehr Munchen (in German).
61. Koide, Y. (2009). Charged lepton mass relations in a supersymmetric Yukawaon model. *Physical Review D—Particles, Fields, Gravitation, and Cosmology, 79*(3), 033009.
62. Joshipura, A. S., & Patel, K. M. (2011). Fermion masses in SO (10) models. *Physical Review D—Particles, Fields, Gravitation, and Cosmology, 83*(9), 095002.
63. Chung, D. Y. (2014). The Periodic Table of Elementary Particles Based on String Theory. *Journal of Modern Physics, 5*, 1234–1243.
64. Fevre, R. (2023). Elementary particle masses: Alternative model to the BEH mechanism. *European Journal of Applied Sciences, 11,* 626–636.
65. Consiglio, J. (2012). On Particle Mass and the Universons Hypothesis. *Applied Physics Research, 4*(2), 144-158.
66. Rodrigues Jr, W. A., &Vaz Jr, J. (1998). From electromagnetism to relativistic quantum mechanics. *Foundations of Physics, 28*(5), 789-814.
67. Namsrai, Kh. (2001). Square-root quantization of elementary particle masses and charges The Abdus Salam International Centre for Theoretical Physics Internal Report IC/IR/2001/18.
68. Bukalov A V 2015 The masses of elementary particles and superconductivity. Part 2 Physics of consciousness and life, cosmology and astrophysics 15(3) 24–7 (in Russian).
69. Bukalov A V 2015 The masses of elementary particles and superconductivity. Part 1 Physics of Consciousness and Life, Cosmology and Astrophysics 15(2) 23–6 (in Russian).
70. Bukalov, A. V. (2015). Periodic law of the mass spectrum of elementary particles in a cosmological model with superconductivity. *Physics of Consciousness and Life, Cosmology and Astrophysics , 15* (4), 18-20.
71. Tatischeff, B., &Brissaud, I. (2010). Relations between elementary particle masses. *arXiv preprint arXiv:1005.0238.*
72. Barak, S. (2019). The Essence of the Elementary Charge and the Derivation and Calculation of the Electron Inertial Mass. *Applied Physics Research, 11*(4), 26-40.
73. Shpenkov G P 2014 Lecture 11: The mass spectrum of elementary particles Dialectical View of the World: The Wave Model (Selected Lectures). 3(2), 135-151.
74. Singh, R. J. (2014). Charges, masses of elementary particles and their structures. *International Journal of Physics and Mathematical Sciences, 4*(1), 102-112.
75. Krolikowski, W. (2005). Excellent approximate solution to the mysterious mass equation by Koide. *arXiv preprint hep-ph/0508039.*
76. Królikowski, W. (2008). Predicting the tauon mass. *arXiv preprint arXiv:0812.1875.*
77. Morisi, S., Peinado, E., Shimizu, Y., & Valle, J. W. F. (2011). Relating quarks and leptons without grand unification. *Physical Review D—Particles, Fields, Gravitation, and Cosmology, 84*(3), 036003.
78. Greulich, K. O. (2010). Calculation of the masses of all fundamental Elementary Particles with an accuracy of approx. 1%. *Journal of Modern Physics, 1*(5), 300-302.
79. El Naschie, M. S. (2003). Non-linear dynamics and infinite dimensional topology in high energy particle physics.

Chaos, Solitons & Fractals, 17(2-3), 591-599.
80. Giudice, G. F. (1992). A New ansatz for quark and lepton mass matrices. *arXiv preprint hep-ph/9204215*.
81. McKeen, D., Rosner, J. L., &Thalapillil, A. M. (2007). Masses and mixings in a grand unified toy model. *Physical Review D—Particles, Fields, Gravitation, and Cosmology, 76*(7), 073014.
82. Mohanta, G., & Patel, K. M. (2023). Gauged SU (3) F and loop induced quark and lepton masses. *Journal of High Energy Physics, 2023*(10), 1-25.
83. King, S. F., Morisi, S., Peinado, E., & Valle, J. W. (2013). Quark–lepton mass relation in a realistic A4 extension of the Standard Model. *Physics Letters B, 724*(1-3), 68-72.
84. Kotkov, A. A. (2016). Mass-spectrum of Charged Leptons from the Planck Mass.
85. Nottale, L. (1994). Scale relativity, fractal space-time and quantum mechanics. *Chaos, Solitons & Fractals, 4*(3), 361-388.
86. Nottale, L. (2004, August). The Theory of Scale Relativity: Non-Differentiable Geometry and Fractal Space-Time. In *AIP Conference Proceedings* (Vol. 718, No. 1, pp. 68-95). American Institute of Physics.
87. Shpenkov, G. P. (2014). Lecture 12: The masses at exchange Dialectical View of the World: The Wave Model (Selected Lectures) 3(2), 152–162.
88. Terazawa, H., &Yasuè, M. (1993). A simple relation among the charged lepton masses. *Physics Letters B, 307*(3-4), 383-386.
89. Terazawa, H. (1989). Supersymmetry in composite models and the mass spectrum of quarks and leptons. In Perspectives on Particle Physics: From Mesons and Resonances to Quarks and Strings Festschrift in Honor of Professor H Miyazawa (pp. 193-204).
90. Fritzsch, H., & Xing, Z. Z. (2000). Mass and flavor mixing schemes of quarks and leptons. *Progress in Particle and Nuclear Physics, 45*(1), 1-81.
91. Mac Gregor, M. H. (2005). Electron Generation of Leptons and Hadrons with Conjugate α-Quantized Lifetimes and Masses. *International Journal of Modern Physics A, 20*(04), 719-798.
92. Gsponer, A., &Hurni, J. P. (2002). Non-linear field theory for lepton and quark masses. *arXiv preprint hep-ph/0201193.*
93. Yu, H., & Ma, B. Q. (2018). Origin of fermion generations from extended noncommutative geometry. *International Journal of Modern Physics A, 33*(29), 1850168.
94. Koide, Y. (1990). Charged Lepton Mass Sum Rule from U (3)-Family Higgs Potential Model. *Modern Physics Letters A, 5*(28), 2319-2324.
95. Koide, Y. (2005). Challenge to the mystery of the charged lepton mass formula. *arXiv preprint hep-ph/0506247.*
96. Foot, R. (1994). A note on Koide's lepton mass relation. *arXiv preprint hep-ph/9402242.*
97. Kocik, J. (2012). The Koide lepton mass formula and geometry of circles. *arXiv preprint arXiv:1201.2067.*
98. Giudice, G. F., & Lebedev, O. (2008). Higgs-dependent Yukawa couplings. *Physics Letters B, 665*(2-3), 79-85.
99. Müller, H. (2010). Fractal scaling models of natural oscillations in chain systems and the mass distribution of the celestial bodies in the solar system. *Progress in Physics, 1*, 62-66.
100. Porshnev, P. I. (2022). Generation of Lepton Masses Complementary to Higgs. *Journal of High Energy Physics, Gravitation and Cosmology, 9*(1), 142-167.
101. Hansson, J. (2014). Physical origin of elementary particle masses. *arXiv preprint arXiv:1402.7033.*
102. Weinberg, S. (2020). Models of lepton and quark masses. *Physical Review D, 101*(3), 035020.
103. Szpiro G G 2003 Chapter 5. Twelve's company, thirteen's a crowd Kepler's Conjecture: How Some of the Greatest Minds in History Helped Solve One of the Oldest Math Problems in the World 1st ed (Hoboken, NJ: Wiley) pp 72–81.
104. Brass, P., Moser, W. O., &Pach, J. (2005). *Research problems in discrete geometry* (Vol. 18). New York: Springer.
105. Teich, E. G., Van Anders, G., Klotsa, D., Dshemuchadse, J., &Glotzer, S. C. (2016). Clusters of polyhedra in spherical confinement. *Proceedings of the National Academy of Sciences, 113*(6), E669-E678.
106. Sagan, F., &Mitoraj, M. P. (2019). Kinetic and potential energy contributions to a chemical bond from the charge and energy decomposition scheme of extended transition state natural orbitals for chemical valence. *The Journal of Physical Chemistry A, 123*(21), 4616-4622.
107. Filippov, A. T. (2010). *The versatile soliton.* Springer Science & Business Media.
108. Infeld E and Rowlands G 2000 Exact methods for fully nonlinear waves and solitons Nonlinear Waves, Solitons and Chaos 2nd ed (Cambridge, UK: Cambridge University Press) p 123.
109. Adam, C., Klimas, P., Sanchez-Guillen, J., &Wereszczyński, A. (2009). Compact shell solitons in K field theories. *Journal of mathematical physics, 50*(10).
110. Belyaeva, T. L., Serkin, V. N., Agüero, M. A., Hernandez-Tenorio, C., &Kovachev, L. M. (2011). Hidden features of the soliton adaptation law to external potentials: optical and matter-wave 3D nonautonomous soliton bullets. *Laser physics, 21,* 258-263.
111. Hsu, L., & Hsu, J. P. (2012). The physical basis of natural units and truly fundamental constants. *The European Physical Journal Plus, 127*, 1-9.
112. Avadhanulu, M. N., Pande, S. A., Golhar, A. R., &Giriya, M. (2022). Applied Physics SemesterI (RTM) Nagpur University 1, 57.
113. Bader, R. F. W. (1970). The hydrogen atom: The probability distribution of the hydrogen atom An Introduction to the Electronic Structure of Atoms and Molecules (Toronto, CA: Clarke, Irwin).
114. Shanks, D., & Wrench, J. W. (1962). Calculation of π to 100,000 decimals. *Mathematics of Computation, 16*(77), 76-99.
115. Harris, J. W., &Stöcker, H. (1998). *Handbook of mathematics and computational science*. Springer Science & Business Media.
116. Amelino-Camelia, G. (2010). Doubly-special relativity: Facts, myths and some key open issues. *Symmetry, 2*(1), 230-271.
117. Premović, P. I. Special Relativity "Meets" the Uncertainty Principle.

118. Hawley, J. F., & Holcomb, K. A. (2005). *Foundations of modern cosmology*. Oxford University Press.
119. Harrison, D. M. (2007). General theory of relativity (University of Toronto).
120. Maljian, L. A. (2023). Introductory astronomy and cosmology: Phys 202: Fall 2023: Third examination lecture notes (New Jersey Institute of Technology).
121. Zheng, X. H., & Zheng, J. X. (2020). Snell's law for the Schwarzschild black hole. *Physical Review D, 102*(10), 104049.
122. Anderson, J. L. (2003). Relativity, General. *Encyclopedia of Physical Science and Technology 3rd ed*, 93-116.
123. Altman, D. G., & Bland, J. M. (2005). Standard deviations and standard errors. *BMJ, 331*(7521), 903.
124. Particle Data Group, Workman, R. L., Burkert, V. D., Crede, V., Klempt, E., Thoma, U., ... &Quadt, A. (2022). Review of particle physics. *Progress of theoretical and experimental physics, 2022*(8), 083C01.
125. Radu, A. (2011). Comment on" Calculation of the Masses of All Fundamental Elementary Particles with an Accuracy of Approx. 1%"[Journal of Modern Physics, 2010, 1, 300-302]. *arXiv preprint arXiv:1102.2815.*
126. Mac Gregor, M. H. (2006). A"Muon Mass Tree" with alpha-quantized Lepton, Quark and Hadron Masses. *arXiv preprint hep-ph/0607233.*
127. Krolikowski, W. (2005). Predicting the tauon mass as well as the ratio of electron and muon masses. *arXiv preprint hep-ph/0509043.*
128. Fianchini, M., & Mikhailov, O. V. (2022). Introduction from Guest Editors to Special Issue "Multi-Metallic Systems: From Strong Cooperative Bonds to Weak MM Interactions". *International Journal of Molecular Sciences, 23*(19), 10998.
129. Rehr, J. J., Zaremba, E., & Kohn, W. (1975). van der Waals forces in the noble metals. *Physical Review B, 12*(6), 2062.
130. Sethi, M. S., &Satake, M. (2010). *Chemical bonding*. Discovery Publishing House.
131. Cahn, R. W., &Haasen, P. (Eds.). (1996). *Physical metallurgy* (Vol. 1). Elsevier.
132. Niebel, K. F., & Venables, J. A. (1974). An explanation of the crystal structure of the rare gas solids. *Proceedings of the Royal Society of London. A. Mathematical and Physical Sciences, 336*(1606), 365-377.
133. Tsai, A. P. (2008). Icosahedral clusters, icosaheral order and stability of quasicrystals—a view of metallurgy. *Science and Technology of Advanced Materials, 9*(1), 013008.
134. Uppenbrink, J., & Wales, D. J. (1992). Structure and energetics of model metal clusters. *The Journal of chemical physics, 96*(11), 8520-8534.
135. Amano, C. (2016). Vibrational Zero-Point Energies and Structures of Rare-Gas Clusters. *Science journal of Kanagawa University, 27*, 3-7.
136. Nelli, D., Roncaglia, C., Ferrando, R., Kataya, Z., Garreau, Y., Coati, A., ... &Andreazza, P. (2023). Sudden collective atomic rearrangements trigger the growth of defect-free silver icosahedra. *Nanoscale, 15*(46), 18891-18900.
137. Plessow, P. N. (2020). The transformation of cuboctahedral to icosahedral nanoparticles: atomic structure and dynamics. *Physical Chemistry Chemical Physics, 22*(23), 12939-12945.
138. Gao, W., Wu, J., Yoon, A., Lu, P., Qi, L., Wen, J., ... &Zuo, J. M. (2017). Dynamics of transformation from platinum icosahedral nanoparticles to larger FCC crystal at millisecond time resolution. *Scientific reports, 7*(1), 17243.
139. McCaw, C. S. (2015). *Orbitals: with applications in atomic spectra.*
140. Orchin, M., Macomber, R. S., Pinhas, A. R., & Wilson, R. M. (2005). T*he vocabulary and concepts of organic chemistry.* John Wiley & Sons.
141. Clouet, E., Varvenne, C., & Jourdan, T. (2018). Elastic modeling of point-defects and their interaction. *Computational Materials Science, 147,* 49-63.
142. Roberts, C. D. (2023). Origin of the proton mass. In *EPJ Web of Conferences* (Vol. 282, p. 01006). EDP Sciences.
143. Faddeev, L. D. (1999). From Yang-Mills field to solitons and back again. *arXiv preprint hep-th/9901037.*
144. Colin, S., Durt, T., & Willox, R. (2017). de Broglie's double solution program: 90 years later. *arXiv preprint arXiv:1703.06158.*
145. Douchin, F., &Haensel, P. (2001). A unified equation of state of dense matter and neutron star structure. *Astronomy & Astrophysics, 380*(1), 151-167.
146. Sala, G., Haberl, F., José, J., Parikh, A., Longland, R., Pardo, L. C., & Andersen, M. (2012). Constraints on the mass and radius of the accreting neutron star in the Rapid Burster. *The Astrophysical Journal, 752*(2), 158.
147. Mongan, T. R. (2020). Standard Model Particles with Mass Treated as Spheres with Finite Radii. *Journal of Modern Physics, 11*(12), 1993-1998.
148. Mac Gregor, M. H. (2006). The top quark to electron mass ratio m (t)= 18* m (e)/alpha^ 2 where alpha= e^ 2/hslash*c. arXiv preprints hep-ph/0603201.
149. Belfatto, B., Beradze, R., &Berezhiani, Z. (2020). The CKM unitarity problem: A trace of new physics at the TeV scale? *The European Physical Journal C, 80*(2), 149.
150. Frey, B., Van Schie, A., &Zacheo, G. (2022, August). Pi-Experience–Making 62.8 Trillion Digits Come Alive. In *Proceedings of the 15th International Symposium on Visual Information Communication and Interaction* (pp. 1-4).
151. Hundi, R. S., &SenGupta, S. (2013). Fermion mass hierarchy in a multiple warped braneworld model. *Journal of Physics G: Nuclear and Particle Physics, 40*(7), 075002.

Supplementary Materials

Supplementary materials (three supplements mentioned in the text of the article) are on this link: https://drive.google.com/drive/folders/10AiCvOHuQEZy-cHhf2SNAhaVUBdY1Whr?usp=drive_link

Note: supplements are traditionally not the subject of editorial assessment (checking). I guarantee the quality of the supplementary information (it contains algorithm, input random values and obtained data (raw), relevant to the work).